

MICROCOPY RESOLUTION TEST CHART  
NATIONAL BUREAU OF STANDARDS-1963-A



REPORT DOCUMENTATION PAGE		READ INSTRUCTIONS BEFORE COMPLETING FORM
1. REPORT NUMBER AFIT/CI/NR 86- 87T	2. GOVT ACCESSION NO.	3. RECIPIENT'S CATALOG NUMBER
4. TITLE (and Subtitle) Model Simulation of a Localized High Intensity Heat Source Interacting with Cooled Metal Plates		5. TYPE OF REPORT & PERIOD COVERED THESIS/DISSERTATION
		6. PERFORMING ORG. REPORT NUMBER
7. AUTHOR(s) Frank Mark Cranfill		8. CONTRACT OR GRANT NUMBER(s)
9. PERFORMING ORGANIZATION NAME AND ADDRESS AFIT STUDENT AT: University of Kentucky		10. PROGRAM ELEMENT, PROJECT, TASK AREA & WORK UNIT NUMBERS
11. CONTROLLING OFFICE NAME AND ADDRESS AFIT/NR WPAFB OH 45433-6583		12. REPORT DATE 1986
		13. NUMBER OF PAGES 83
14. MONITORING AGENCY NAME & ADDRESS (if different from Controlling Office)		15. SECURITY CLASS. (of this report) UNCLAS
		15a. DECLASSIFICATION/DOWNGRADING SCHEDULE
16. DISTRIBUTION STATEMENT (of this Report) APPROVED FOR PUBLIC RELEASE; DISTRIBUTION UNLIMITED		
17. DISTRIBUTION STATEMENT (of the abstract entered in Block 20, if different from Report)		
18. SUPPLEMENTARY NOTES APPROVED FOR PUBLIC RELEASE: IAW AFR 190-1		<p><b>DTIC ELECTED</b></p> <p><b>S</b> <i>Star</i> <b>D</b></p> <p>AUG 13 1986</p> <p><b>E</b></p> <p><i>Lynn E. Wolaver</i> LYNN E. WOLAVER 6 AUG 12 Dean for Research and Professional Development AFIT/NR</p>
19. KEY WORDS (Continue on reverse side if necessary and identify by block number)		
20. ABSTRACT (Continue on reverse side if necessary and identify by block number)  ATTACHED.		

AD-A170 856

DTIC FILE COPY

MODEL SIMULATION OF A LOCALIZED HIGH INTENSITY HEAT SOURCE INTERACTING  
WITH COOLED METAL PLATES

THESIS

A thesis submitted in partial fulfillment of the  
requirements for the degree of Master of Science in  
Nuclear Engineering at the University of Kentucky

By

Frank Mark Cranfill

Lexington, Kentucky

Director: Dr. O.J. Hahn, Professor of Mechanical Engineering

Lexington, Kentucky

1986



Accession For	
NTIS GRA&I	<input checked="" type="checkbox"/>
DTIC TAB	<input type="checkbox"/>
Unannounced	<input type="checkbox"/>
Justification	
By _____	
Distribution/	
Availability Codes	
Dist	Avail and/or Special
A-1	

## ABSTRACT OF THESIS

### MODEL SIMULATION OF A LOCALIZED HIGH INTENSITY HEAT SOURCE INTERACTING WITH COOLED METAL PLATES

The basic, generic problem of a localized high intensity heat source directed against one surface of a plate of finite thickness was investigated using the finite element program ANSYS by Swanson Analysis Systems, Inc. After reviewing similar work in nuclear fuel and laser machining, ANSYS was verified against a known solution. ANSYS was used to create a model that yields minimum heat transfer coefficients needed to prevent the initiation of melting in thin aluminum, titanium, and stainless steel (AISI 304) plates. These heat transfer coefficients were converted into minimum local Nusselt numbers and graphed against local Nusselt number correlations for constant temperature flat plates in forced and free convection regimes. A detailed listing of both laminar and turbulent correlations is presented along with references. The suitability of liquid sodium, air, and water (under high pressure) as coolants for a source intensity of  $2.0 \times 10^7 \text{ W/m}^2$  was examined. For free convection, only liquid sodium cooling a titanium plate is feasible. For forced convection, liquid sodium is feasible in laminar flow for all three plates with velocities ranging from 0.28 m/s to 1.09 m/s. Water is feasible for aluminum and titanium in turbulent flow at velocities of approximately 4 m/s.

*Frank Mark Cranfill*

Frank Mark Cranfill

*30 May 1986*

30 May 1986

MODEL SIMULATION OF A LOCALIZED HIGH INTENSITY HEAT SOURCE INTERACTING  
WITH COOLED METAL PLATES

By

Frank Mark Cranfill

*C. J. Hahn*

\_\_\_\_\_  
(Director of Thesis)

*C. J. Hahn*

\_\_\_\_\_  
(Director of Graduate Studies)

*30 May 1986*

\_\_\_\_\_  
(Date)

THESIS

Frank Mark Cranfill

The Graduate School  
University of Kentucky

1986

MASTER'S THESIS RELEASE

            
  X    
          

I authorize the University of Kentucky Libraries to reproduce this thesis in whole or in part for purposes of research.

I do not authorize the University of Kentucky Libraries to reproduce this thesis in whole or in part for purposes of research.

Signed:

Frank Mark Caspell

Date:

30 May 1986

## ACKNOWLEDGEMENTS

First and foremost, I would like to express my appreciation to General Bennie L. Davis, former Commander in Chief of the Strategic Air Command, in selecting me for the Senior Commander's Education Program. It was this assignment that made coming to the University of Kentucky possible in the first place.

Second, I am indebted to my advisor, Dr. O.J. Hahn for providing the impetus for this work. His knowledge and vision formulated the major guidelines that this work followed. Also, I would like to thank Dr. K.E. Rouch for suggesting the use of the finite element analysis program ANSYS as the basis for my model. His expertise and direction were instrumental in constructing and debugging the model. In addition, Mr. David Johnson of Swanson Analysis Systems, Inc., deserves a special thanks for his suggestions and answered questions concerning ANSYS.

Third, and most important as far as the computer model is concerned, I would like to thank the Harris Corporation for their donation of a Harris 800 Computer to the University of Kentucky Engineering Computer Center. This donation allowed me to use at least 270 CPU hours without concern for cost (which could have amounted to almost \$80,000 normally). Also, a special thanks is due Scott Sendlein, Director of Engineering Computing, for giving me four accounts on the Harris 800 (and thus expediting the work) as well as answering a myriad of questions.

Fourth, the collective staffs of three separate University of Kentucky departments deserve special acknowledgement: 1) the Engineering Computer Center staff for their assistance and especially for staying after hours on a couple of occasions allowing me to complete

critical jobs; 2) the Engineering Library Staff (especially Mr. Russell H. Powell) for their assistance in tracking down journals and running literature searches; and 3) the Government Publications staff of the M.I. King Library - the most helpful and efficient organization I have ever encountered.

Fifth, I would like to thank Dr. Richard I. Kermode for serving on my examination committee. Also, a number of people deserve special thanks for loaning me references from their personal libraries as well as helpful advice and discussions: Dr. Raschid Bhatti, Dr. C.J. Cremers, Dr. V. Vedhanayagam, Mr. Rajendra K. Arora, Mr. Michael Atogi, Mr. Vibhas Chandrachood, Mr. Dana Graves, Mr. Alan Holt, Mr. Ralph Joseph, Mr. Matthew Marsh, Mr. Martin Pais, and Mr. Sanjay Pandita. Additionally, I would like to thank Mrs. Ernestine Barnes for consenting to type this thesis.

Sixth, I would like to express my heart-felt gratitude to my wife, Susan, for her patience and love and for virtually raising our three children single-handedly during our stay here--thus allowing me the necessary time for this work. I would additionally like to thank my children--John, Cindy and Julie--for their understanding and love during this work. Also, a special thanks to my mother, Mary Cranfill, for her help in producing the first draft of this thesis. Furthermore, a very special thanks to my brother, John E. Cranfill, for putting in many hours of cataloging the multitude of computer printouts produced by this model as well as spending a number of hours proof-reading the text.

Finally, I would be extremely remiss if I did not offer, in writing, my deepest appreciation to God--who I sincerely believe made all of the above, as well as this work, possible.

## TABLE OF CONTENTS

	<u>Page</u>
ACKNOWLEDGMENT .....	iii
TABLE OF CONTENTS .....	v
LIST OF TABLES .....	viii
LIST OF FIGURES .....	ix
NOMENCLATURE .....	xi
CHAPTER	
I. Introduction .....	1
II. Background .....	6
2.1 Introduction .....	6
2.2 Representative Work in Nuclear Fuel .....	7
2.3 Representative Work in Laser-Machining .....	11
III. Model Development .....	16
3.1 Preliminaries .....	16
3.2 ANSYS .....	18
3.3 Verification of ANSYS .....	20
3.4 Defining Model Parameters .....	24
IV. Numerical Solutions and Correlation Results .....	27
4.1 Presentation of Numerical Solutions .....	27
4.1.1 Heat Transfer Coefficient as a Function of Heat Source Intensity .....	27
4.1.2 Heat Transfer Coefficient as a Function of Affected Area at Various Intensities .....	31
4.1.3 Heat Transfer Coefficient as a Function of Thickness in Aluminum .....	35

4.1.4	Heat Transfer Coefficient as a Function of Conductivity .....	37
4.2	Nusselt Number Correlations for Free and Forced Convection .....	37
4.2.1	Nusselt Number Correlations for Free Convection .....	39
4.2.1.1	Free Convection--Laminar--Flow Constant Temperature .....	40
4.2.1.2	Free Convection--Turbulent Flow-- Constant Temperature.....	41
4.2.2	Nusselt Number Correlations for Forced Convection .....	42
4.2.2.1	Forced Convection--Laminar Flow -- Constant Temperature .....	43
4.2.2.2	Forced Convection--Turbulent Flow-- Constant Temperature .....	44
4.3	Cooling Condition Determination and Coolant Evaluation Results .....	44
4.3.1	Forced Convection Results .....	45
4.3.2	Free Convection Results .....	55
IV.	Conclusions and Further Study .....	61
5.1	Conclusions.....	61
5.2	Further Study Recommendations .....	62

APPENDICES

A.	Sample Computer Program Used to Test Accuracy of ANSYS....	63
B.	Sample Computer Program for Determining Minimum Heat Transfer Transfer Coefficient .....	67
C.	Minimum Heat Transfer Coefficients Necessary to Prevent Melting at Various Intensities.....	69
D.	Data for Figures 2-4.....	70
E.	Minimum Heat Transfer Coefficient as a Function of Thickness .....	73
F.	Data for Heat Transfer Coefficients as a Function of Conductivity.....	74

G. Error Analysis Overview.....	75
REFERERENCES .....	77
VITA .....	83

LIST OF TABLES

Table	Page
1. Test Runs to Establish Accuracy of ANSYS Model.....	23
2. Minimum Local Nusselt Numbers .....	46

## LIST OF FIGURES

Figure	Page
1. Minimum heat transfer coefficient $[h(x)]$ plotted as a function of localized heat source intensity for aluminum, stainless steel, and titanium plates, 0.0004 m thick .....	28
2. Minimum heat transfer coefficients for aluminum plotted as functions of area affected by a localized high intensity heat source at intensities of $1 - 6 \times 10^7 \text{ W/m}^2$ .....	32
3. Minimum heat transfer coefficients for stainless steel plotted as functions of area affected by a localized high intensity heat source at intensities of $1 - 6 \times 10^7 \text{ W/m}^2$ .....	33
4. Minimum heat transfer coefficients for titanium plotted as functions of area affected by a localized high intensity heat source at intensities of $1 - 6 \times 10^7 \text{ W/m}^2$ .....	34
5. Minimum heat transfer coefficient $[h(x)]$ required for cooling an aluminum plate plotted as a function of thickness of the plate.....	36
6. Minimum heat transfer coefficient versus each metal's conductivity (titanium, stainless steel, and aluminum) for the case of heat intensity = $2 \times 10^7 \text{ W/m}^2$ .....	38
7. The minimum Nusselt numbers required to prevent melting in each metal plate are plotted versus Reynolds number to demonstrate how the graph is constructed.....	48
8. The turbulent and laminar Nusselt number correlations are plotted to demonstrate both the large difference in the correlations as well as the construction of the combined figure...	49
9. The combined figure for sodium as the coolant results from overlaying Figure 7 on Figure 8 .....	50
10. The combined minimum Nusselt numbers and turbulent and laminar Nusselt number correlations for air.....	52
11. The special case of water under high pressure ( $1.235 \times 10^7 \text{ N/m}^2$ and $Pr = 1.0$ ) cooling aluminum subjected to a $2 \times 10^7 \text{ W/m}^2$ localized heat source.....	53
12. The special case of water under very high pressure ( $2.152 \times 10^7 \text{ N/m}^2$ and $Pr = 12.0$ ) cooling titanium subjected to a $5 \times 10^7 \text{ W/m}^2$ localized heat source.....	54
13. Nusselt number versus Grashof number for water under high pressure ( $1.235 \times 10^7 \text{ N/m}^2$ ) cooling aluminum by free convection.....	57

14. The combined minimum Nusselt number lines for aluminum, stainless steel, and titanium are plotted with the laminar correlation applicable to free-convection cooling with liquid sodium..... 59

## NOMENCLATURE

A	parameter related to Prandtl number in the Eckert and Drake [73] correlation for forced convection -- turbulent flow -- constant temperature
a	unknown in quadratic temperature function used by ANSYS
b	unknown in quadratic temperature function used by ANSYS
c	unknown in quadratic temperature function used by ANSYS
$c_p$	specific heat at constant pressure
$C_1$	arbitrary constant
[C]	specific heat matrix
exp( )	e raised to the power of the quantity in ( )
F	peak amplitude value
F(r)	amplitude of Gaussian distribution
g	gravitational constant
Gr(x)	local Grashof number
h(x)	local heat transfer coefficient
k	thermal conductivity
$k_f$	thermal conductivity of the fluid (coolant)
[K]	thermal conductivity matrix
L	thickness of plate
Nu(x)	local Nusselt number
Pr	Prandtl number
$q_x$	heat flux from plate in x-direction
(Q)	heat flow rate vector
( $Q_t$ )	heat flow rate vector at time t
r	radial distance in Gaussian distribution
Re(x)	local Reynolds number

$t$	time
$T_B$	temperature on the back face of the plate (opposite the high intensity heat source)
$T_F$	temperature on the front face of the plate (same side as high intensity heat source)
$T_m$	melting point temperature
$T_S$	temperature of the back face of the plate for free convection computations
$T_t$	temperature at time $t$
$T_\infty$	free stream temperature of the coolant
$\Delta t$	time step between iterations in ANSYS program
$(T)$	nodal temperature vector
$(\dot{T})$	time rate of change in nodal temperature vector
$(T_t)$	nodal temperature vector at time $t$
$u_{fs}$	free-stream velocity
$x$	distance (usually from leading edge of plate)
$\beta$	volumetric expansion coefficient
$\rho$	density
$\sigma$	standard deviation
$\nu$	kinematic viscosity

## Chapter 1

### INTRODUCTION

The objective of this work is to investigate the basic problem of a localized high intensity heat source directed against one surface of a plate of finite thickness and cooled on the other surface by free or forced convection. The applicability of this problem extends across a wide variety of fields. In the nuclear industry this situation is known as the 'hot-spot' problem and is encountered in various fuel assemblies, particularly fuel pellets. In industries that use laser machining, the applications include possible cooling problems encountered during cutting, drilling, or welding. In the defense industry, with the advent of lasers as viable weapons, the problem extends to the development of possible defensive measures incorporating various cooling systems. In the space industry, possible applications include the minimization of laser effects on satellites as well as the study of 'hot spot' development during the burning of solid rocket fuel. Other possible applications include: cooling requirements of energy collectors for solar power; the study of cooling effects on electrical arcing and conductor diameter variation; and local heat generation in gun barrels due to raised spots. Additionally, the basic problem in all these fields can include a localized high intensity heat source superimposed over an already existing heat flux or temperature field. In any case, all of the above examples include the presence of a localized high intensity heat source where cooling requirements must be determined. Thus, a computer model that addresses a part of this basic problem would prove very useful. Such a model is presented here, with the above applications simplified to examining the case of a thin vertical metal

plate subjected to steady-state heating conditions.

The specific question this computer model is designed to answer is: what minimum heat transfer coefficient is needed to prevent a localized high intensity heat source from initiating melting on the front face of a metal plate assuming only the back face of the plate is cooled? The data assumed known is: the intensity of the heat source; the area of the front face of the plate affected by the heat source; the thickness of the plate; and the thermal properties of the plate. A proposed heat transfer coefficient is supplied by the user, and the model then provides the top ten temperatures (based on node location from a finite element program) on the front and back faces of the plate in order to determine if melting would occur and to analyze cooling conditions. The user continues to adjust the value of the proposed heat transfer coefficient until the maximum temperature on the front face is just below the melting point of the material under examination. Since the front surface of the plate outside of the affected area of the heat source is considered to be adiabatic, including the plate edges, the resulting heat transfer coefficient represents an upper-bound value of the minimum cooling required to prevent the initiation of melting on the front face. This resulting minimum heat transfer coefficient is used to determine the feasibility of potential coolants. The latitude available to the user in varying the material of the plate is limited only by his knowledge of its thermal properties. The limitations on the dimensions of the plate were not fully investigated. A 0.05 m square plate was used in the testing of the model with a thickness of 0.0004 m. The model was verified for thicknesses of up to 0.0032 m in the case of aluminum. Further investigation was precluded by time constraints.

The two main fields that generated interest in and contributed most to the development of this model are nuclear fuel and laser machining. Thus their applications of the model will be explored in detail. In nuclear fuel, the effect of 'hot spots' in fuel elements can be modelled by estimating worst-case heat intensities from contact of the fuel with the cladding. (This contact results from pellet cracking and relocation as well as fuel deformation that occur during normal operation of the reactor.) These intensity estimates plus representative values of cooling-fluid flow and cladding thickness can then be entered into the model. To provide this information to the program requires experimental or calculated data of typical heat intensities due to 'hot spots' in fuel elements. Fortunately, much data applicable to this problem has already been published in the form of contact conductance values [1-7]. Worst-case heat intensities can then be calculated by multiplying these experimental contact conductances by estimated worst-case temperature distributions obtained from either accident condition studies or normal operation studies. Characteristic temperatures can thus be either calculated from current reactor models [8-12] or obtained directly from test data [12-14]. Thus, with these data, the computer model can determine the new cooling conditions necessary to prevent the cladding from melting due to 'hot spots' in the pellets.

In laser machining, the model is especially applicable to laser drilling. By assuming free-convection cooling on the backside of the plate, the model takes on the form of a laser-drilling problem with the localized high intensity heat source representing the laser beam. The model does not take into account the effect of laser induced plasma; but as noted by Herziger [15], the undesirable properties of the laser

induced plasma cloud can be avoided (or at least minimized) by using an appropriate pulse program for pulsed lasers. For continuous wave (cw) lasers, experiments demonstrate that machining with them is only of advantage in a few cases, preferably when the generation of laser induced plasma can be avoided. So neglecting the effects of laser induced plasma on the model does not invalidate its usefulness to the area of laser drilling and at the same time maintains the model's generic nature.

In the following study, a review of some of the similar work done in nuclear fuel and laser machining is presented. Then the rationale is given for choosing the finite element package, ANSYS, by Swanson Analysis Systems, Inc. as the basis for the model. The basic principles behind the operating procedures of ANSYS are summarized and the program is verified by a comparison run against analytical data provided by Torvik [16]. Though the basic problem being investigated includes flat plates, walls of cylinders, and walls of spheres, only the case of the vertical flat plate is examined. Aluminum, titanium, and AISI 304 stainless steel plates are examined under steady-state heating conditions in the  $1 \times 10^7$  to  $6 \times 10^7$   $\text{W/m}^2$  range in order to determine the upper bounds of the minimum cooling requirements. The heat transfer coefficients obtained from the model are used, along with local Nusselt number correlations for free and forced convection, to determine the feasibility of air, water, or sodium meeting the minimum cooling requirements for the materials and conditions examined. Relationships of heat transfer coefficient as a function of heat source intensity, area of plate affected by the heat source, and conductivity are presented in graphical and tabular form. Heat transfer coefficient as a

function of thickness is also presented for aluminum. Finally, recommended areas for further study are presented.

## Chapter 2

### BACKGROUND

#### 2.1 Introduction

The generic problem of a localized high intensity heat source directed against a vertical flat plate with either free or forced convection cooling on the opposite side has received only partial coverage in the literature. In fact, two separate literature searches-- one of nuclear fuel and one of laser machining--produced no direct handling of the problem. The literature search of nuclear fuel involved the DOE Energy Database extending back through 1974. The search of laser machining involved the DOE Energy Database extending back through 1974; the Metadex Database back through 1966; the Compendex Database back through 1970; and the Dissertation Abstracts Online Database back through 1961. The work done in the laser material processing field deals almost exclusively with a localized high intensity heat source directed on a flat plate (vertical or horizontal), but cooling on the opposite side of the plate is not considered (backside is either infinite or adiabatic). In the nuclear field, most of the work centers around determining the conductance of the gap between the fuel pellet and its cladding. 'Hot spots' arising from relocation of the fuel in the pellet due to normal operation or fuel deformation are treated in either a statistical manner or through the determination of a contact conductance. Clad-to-coolant heat transfer is generally calculated by use of correlations for film coefficients in subroutines of the various computer models of reactor operation. Thus cooling is considered in a generalized, lumped correlation. Melting is considered only as it applies to the fuel since the fuel is generally at much higher

temperatures than the cooled cladding. A summary of representative work in both fields follows.

## 2.2 Representative Work in Nuclear Fuel

Garnier and Begej [17, 18] come close to the generic problem in their study of thermal gap and contact conductance between depleted uranium dioxide ( $UO_2$ ) and Zircaloy-4 (Zr4) using the Modified Pulse Design (MPD) technique. MPD is a transient technique employing a laser heat pulse and a signal detector to monitor the thermal energy transmitted through a  $UO_2/Zr_4$  sample pair which are either in contact or separated. This technique is a modification of the classical heat pulse (flash) method [19] commonly used to determine the thermal diffusivity and conductivity of materials. MPD uses a laser to supply a heat pulse to the front face of a  $UO_2-Zr_4$  sample pair that are in light contact or slightly separated. An intrinsic fast response thermocouple monitors the subsequent rise on the back face of the Zircaloy. Using this transient temperature response and knowledge of the thermal properties of the specimens, the thermal gap conductance is determined as a function of changing variables (i.e. temperature, mean-plane gap width, gas composition, etc.). The mathematical description of MPD is very similar to that of the present work; however, several of its basic assumptions are quite restrictive. In MPD, only one-dimensional heat conduction is considered, due to the experimental assembly construction. Thermal properties of the specimens are considered constant since the temperature transients are no greater than 4°K. The unknown quantities are the heat losses of the front and back faces and the heat transfer across the gap. Laplace Transforms are used on the governing equations

and the very short laser pulse is considered to be a Dirac Delta function. A method developed by Peckham [20], that attempts to minimize the sum of the squared errors, is chosen for determining the unknown parameters. Garnier and Begej conclude that the MPD technique is reliable for gap conductance measurements but not for solid-solid contact conductance due to the difficulty in applying suitable contact pressures to the specimens. They also provide a Fortran program for calculating the best fitting convective coefficients for a given set of data.

Suzuki et. al. [21] present a code which calculates a cooling flow distribution in a reactor vessel and couples it with a code which analyzes temperature distribution in a fuel assembly. Various analytical models for coolant flow distribution in the reactor vessel, for pressure drop calculations, and for temperature distribution calculations in coolant and fuel elements in the assembly are presented in detail. An expression is also given for calculating 'hot spot' temperatures but only through the use of statistical uncertainties in nominal temperature differences. This allows the 'hot spot' temperature to be estimated in some specified assemblies so that operational safety can be confirmed.

Baker [22] refines methods for calculation of fuel temperature in  $\text{PuO}_2\text{-UO}_2$  fuel in Fast Breeder Reactor fuel pins. His primary concern is the calculation of temperature changes across the fuel-to-cladding gap in pins with fuel burnups that range from 60 - 10,900 MWd/MTM (0.006 - 1.12 at.%). He proposes a complete set of heat transfer formulations that include sodium-to-cladding temperature drop, cladding temperature drop, heat transfer across the fuel-to-cladding gap, and heat transfer

across the unrestructured and restructured fuel regions. He also uses a computer code (SIEX-M1) to calibrate the fuel-to-cladding gap conductance model. Calculations of the heat transfer across the fuel-to-cladding gap are based primarily on expressions suggested by Ross and Stoute [23]. The modified model used is briefly described in the documentation of the SIEX computer code [24].

Meek et. al. [25] apply Kalman filter methodology to an in-pile liquid-metal fast breeder reactor simulation experiment to obtain estimates of the fuel clad thermal gap conductance. By using a Kalman filter (a linear minimum-error variance sequential state estimation algorithm) an optimal estimate of the state vector chosen to characterize the experiment is obtained. From this estimate, the fuel-clad thermal gap conductance is calculated as a function of time and axial position along the length of the fuel pin.

Horn and Panisko [10] give a detailed description of the GAPCON code and the different subprograms that are part of it. Of particular interest to the present work is the subroutine used to calculate cladding-to-coolant heat transfer coefficients. If the coolant is water, the calculation is based on the Dittus-Boelter equation [26]. If the coolant is liquid sodium, then the same expression as noted by Baker [22] is used. The program is designed to handle thermal conductivity as a function of temperature, a feature also available on the present work.

Sudoh [11] presents HETFEM, a two-dimensional thermal conductivity analysis code that utilizes a finite element method for analyzing thermal responses of fuel rods during reflood. He develops the partial differential equations and boundary conditions in vector notation for transient heat conduction in solids and uses the method of weighted

residuals to approximate the solution to the problem.

Roberts et. al. [27] present the Performance Analysis and Design (PAD) computer code as an example of a computer code that uses a modified version of the Mikic-Todreas model [28] to calculate gap conductance after pellet-clad contact has been established. The model operates under the assumption that, once contact has been made, the gap conductance is no longer a function of internal pressure.

Marr [29] shows how COBRA-3M was developed to be suitable for analysis of thermal-hydraulics in small pin bundles commonly used in in-reactor and out-of-reactor experiments. It uses detailed thermal circuits models for the fuel pins and duct walls. The model handles temperature dependent properties, nonuniform power distributions and fuel restructuring and melting. COBRA-3M also uses finite difference techniques and one-dimensional (radial) heat flow.

Finally, Nguyen-Minh and Neuer [30] investigate the possibility of using the modulated heating beam method--a well-known technique for measuring thermal diffusivity--for determining thermal gap conductance. They find that if only radiant heat losses are present, it is possible to determine thermal gap resistance merely by measuring the phase lag.

The preceding summary is by no means comprehensive. It is presented here to give the reader an idea of the work being done in the nuclear field pertaining to the determination of heat transfer coefficients and cooling requirements in general. Note should be made that the emphasis of the foregoing studies usually centers on the heat transfer characteristics of the gap between the fuel and cladding. Any work done with melting concerns only the melting point of the fuel since it operates at temperatures much greater than the cooled cladding. The

present work, on the other hand, is more concerned with the cladding since it more closely approximates the "vertical flat plate" of the basic problem. But the data presented in the literature is still valuable to the present work because with the gap conductance values listed and temperature profiles available--worst-case heat intensities can be estimated thus enabling the examination of conditions leading to possible melting of the cladding.

### 2.3 Representative Work in Laser-Machining

In laser-machining, Golodenko and Kuz'michev [31] examine the thermal processes that occur in metals when irradiated by powerful laser pulses. They solve the heat-conduction problem giving due allowance for the motion of the evaporating boundary. An infinite plane metal surface is considered that has been subjected to a uniform surface density of radiant energy from a laser. The results of the calculations for copper are presented in the form of a series of graphs. The results confirm their expectations that, for the same energy on the pulse, the thickness of the evaporated layer is greater for pulses of shorter duration.

Locke et. al. [32] examine deep penetration welding with high-power CO<sub>2</sub> lasers at substantially higher power levels than on all previously reported experiments. Experimental results are presented in graph and table form. The measured penetration for their tests is in reasonably good agreement with established correlations for vacuum electron beam welding [33].

Torvik [16, 34] presents a method for determining the two-dimensional transient temperature distribution and progression of melting on disks subjected to an applied flux over one face. He uses a

finite element method that performs heat balances in the elements over finite time measurements. His method is in good agreement with known solutions to two-dimensional heat conduction problems as well as the one-dimensional melting problem. As a result, the present work draws heavily from Torvik, using his work to help confirm the validity of the present model as well as set up the analyses. Also, Torvik includes in his results a demonstration that the time required for melt-through approaches that for the one-dimensional case if the power per unit thickness is sufficiently large. For future study, it is helpful to note that phase changes can also be incorporated in Torvik's model. In a later numerical study [34], he produces a method for estimating from a single curve the melt-through time for any arbitrary combination of flux, spot size, thickness, and material. Also presented is melt-through time for the case of complete retention of the melt until vaporization as well as predictions for heating due to a large single pulse. Part of Torvik's analysis is used for the purpose of comparison in the present work since it most closely approximates the basic problem under study.

Paek and Gagliano [35] develop a model that uses a continuous, distributed, moving heat source to describe the temperature profile and thermal stress propagation for laser-drilled holes in high-purity fired-alumina ceramic substrate material. In order to indicate the magnitude of those factors influencing the potential fracture of the alumina material, the temperature profile and tangential stress distribution of the laser-formed hole are calculated. Both finite and infinite bodies are considered, and temperature independent properties and no heat losses through the bounding surface are assumed. Reflection losses are

neglected. A very practical result of their work is the ability to predict the profile of the laser-drilled hole. The theory they develop indicates shorter pulse lengths generally give lower stresses and that the desirable condition for hole drilling is to maintain a sufficiently high beam intensity for a minimum time in order to remove by sublimation a given mass of material.

Prokhorov et. al. [36] present experimental and theoretical results on metal evaporation under powerful optical radiation (normal laser pulses with light intensity of approximately  $10^{11}$  W/m<sup>2</sup> and spot size on the target of about 0.01 m). They also review some factors that limit the rise of surface temperature (i.e. instability of superheated liquids, intense boiling of liquid, the disappearance of metal conductivity). Furthermore, they point out that experimental data is already in the literature directly supporting the existence of a sharp drop in reflectivity with increased intensity of light incident on a metal surface [37]. They propose a method for calculating metal surface temperature versus incident light intensity by using an approximate solution to the Clapeyron-Clausius equation. Results of investigating vapor dynamics of metal evaporation under powerful millisecond optical radiation are also reported.

Jones and Wang [38] examine the effect of temperature as a function of time in laser welding of similar and/or dissimilar materials using experiment and finite element analyses. They detail the laser operating parameters as well as the finite element method and temperature dependent properties. Their experimental results show that, with proper operating parameters, good tensile strength and low electrical resistance can be obtained in copper-copper welds. With the addition of

moderate contact pressure, copper-aluminum welds can result in good tensile and impact strength as well as good electrical resistance stability after thermal cycling. For the present work, their use of finite element analysis is the most noteworthy.

Blottner [39] presents a relatively simple numerical technique for predicting the melt depth for pulsed laser welding. He approximates the two-dimensional aspects of the problem by using an effective area in the one-dimensional energy equation. He uses the enthalpy method with an implicit numerical scheme to provide a rapid solution procedure.

Herziger [16] examines the strong coupling between laser and target due to optical feedback from the target that results in changing the system parameters of the laser tool. He studies the processing parameters; factors affecting the absorption of laser radiation; and the effects of laser induced plasma. He concludes that the application of absorptive layers or an appropriate choice of laser parameters for a poor optical absorptivity material can increase its absorptivity to nearly unity. For the present work, this conclusion is used as a basis for neglecting plasma effects. He further concludes that the quality of laser machining depends strongly on the proper adjustments and control of the laser radiation.

Decker et. al. [40] present some primary steps in developing a cutting model. They conclude a cutting model should be as simple as possible and should be able to: give an estimation of the cutting speed; show how the quality of the cutting surface depends on the process parameters; and predict the metallurgical impact on the workpiece. (For the present work, these attributes of a good cutting model were the deciding factors in choosing the work of Torvik [16] as

the basis of comparison since he not only uses finite element analysis but his model addresses cutting speed and the metallurgical impact.) Decker et. al. also list the three different versions of laser cutting as well as the parameters controlling the process (i.e. laser beam, assistant gas, material, slag). The need to optimize the parameters of cutting speed, width, and cutting surface is presented in addition to details on each parameter. The cutting process is thoroughly examined and the report is concluded with a detailed cutting model that considers the dissipation and production of heat energy.

As with nuclear fuel, the above listing is by no means exhaustive. The listing's primary purpose is to give the reader a general overview of work already accomplished in laser-machining that applies to the present work and to some of its possible applications. Additionally, the listing presents a brief introduction to the fundamental nature of the basic problem of localized high intensity heat sources.

## Chapter 3

### MODEL DEVELOPMENT

#### 3.1 Preliminaries

The first decision that had to be made was to choose which computer system to use for development of the model. The logical choice was the University of Kentucky Engineering Computer Center's Harris 800 Computer System. This system had just recently been donated to the college by the Harris Corporation and as a result the computer time was 'free'. With unlimited computer time available coupled with the fact that this model was to provide only the foundation for more in-depth examination of the basic problem, the next decision was to proceed with a three-dimensional model. Most of the literature deals with one- and two-dimensional models due to the normal high expense of computer time and the need for expeditious solutions to engineering problems. With neither of these constraints present, a three-dimensional model would allow the greatest accuracy as well as the greatest versatility since it could examine cases where the one- and two-dimensional approximations would not apply.

With a computer system and dimension chosen, a methodology had to be determined. The most extensively used method is probably the finite difference method. Its use in one-, two-, and three-dimensional models is well documented [41-45], and involves the use of discretization to develop algebraic "difference" equations from the governing equations. Advantages of this numerical method are its familiarity (most computer courses cover finite differences before other numerical methods) and its relative simplicity. A disadvantage of this numerical method, as with any method designed to solely calculate numerical values for

temperatures, is that temperature gradients cannot be determined accurately. Thus, thermal stresses, which depend directly on thermal gradients, cannot be easily calculated. Also, phase change and material inhomogeneities are difficult to model.

Alternatively, the finite element method offers some different features. It too has been well documented in one-, two-, and three-dimensional use [11, 16, 34, 38, 46 - 49], and in addition is advantageous in dealing with inhomogeneous materials and phase changes. Additional advantages of the finite element method over other numerical approaches are listed by Wilson and Nickell [46]. For the finite element method, the body under study is replaced by a system of elements with each element being defined by a pattern of nodes. For heat transfer studies, an approximate solution for each element in the temperature field is assumed and heat flux equilibrium equations are developed within the finite element system at a discrete number of nodes. The algebraic relationships between the nodal temperatures are then solved. For transient problems, the system of equations must be solved for each time step which requires the inversion of a large matrix for each time increment. This can lead to long computer running times but the flexibility of the method more than makes up for this disadvantage.

Weighing the above considerations made the choice of the finite element method the likely result, but the decisive factor was the availability of the finite element program ANSYS by Swanson Analysis Systems, Inc. on the Harris computer. Thus, the combination of a ready-made finite element system and unlimited computer time made finalizing the preliminary decisions a rapid procedure.

### 3.2 ANSYS

The ANSYS computer program is a large-scale, general purpose program for the solution of several varieties of engineering analyses. The program employs the matrix displacement method of analysis based on the finite element idealization. It uses a wave-front (or frontal) solution procedure [50, 51] for the system of simultaneous linear equations developed from the set of finite elements. The wave front at a point is defined as the number of active equations after any element has been processed during the solution procedure. The program is designed to handle up to 2000 degrees of freedom normally, however the version used by universities is a special educational version of ANSYS and is limited to a 200 degree of freedom wave front. This and the limited memory size for node coordinate storage are the only differences between the two versions, but they allow Swanson Analysis Systems, Inc. to lease ANSYS to the schools at a greatly reduced cost.

Though ANSYS is mainly a structural analysis program, it handles heat transfer problems equally well. Its thermal analysis module is used to solve for steady-state or transient temperature distributions in a body. Conduction, convection, radiation, and internal heat generation can all be incorporated in the model along with heat transport effects due to flowing fluids. Material properties may be either constant or temperature dependent, and output temperatures may be stored and used for structural analyses (a feature that will be utilized in future work). Automatic convergence criteria are available for steady-state, nonlinear solutions while a time-step optimization procedure is available for transient solutions. For the present work, both of these

features are demonstrated. The latter one is used to verify the model, while the former is used for the major part of the analysis.

The basic equation for the thermal analysis in ANSYS is Poisson's equation with temperature being the primary unknown. The basic equation is written as:

$$[C](\dot{T}) + [K](T) = (Q)$$

where:

[C] - the specific heat matrix

[K] - the thermal conductivity matrix (including equivalent face convection terms)

(T) - the nodal temperature vector

(Q) - the heat flow rate vector (including applied heat flow, internal heat generation, and convection)

(Note: For the steady-state case, which is the main concern of the present work, the  $(\dot{T})$  term is zero and the equation reduces to:  $[K](T) = (Q)$ .) The basic equation is solved by an implicit direct integration scheme based on a modified Houbolt method. This method uses a quadratic temperature function (where  $T_t$  is the temperature at time  $t$ ) over the region being examined of the form:

$$T_t = a + bt + ct^2$$

The temperature function is differentiated and substituted into the basic equation to yield an equation with three unknowns:  $a, b,$  and  $c$ . If  $\Delta t$  is the time step between iterations, a set of three equations may be defined at  $t, t - \Delta t,$  and  $t - 2\Delta t$ . These equations are then solved simultaneously to give the integration equation:

$$\left[ \frac{C_1}{\Delta t} [C] + [K] \right] (T_t) = (Q_t) + f([C], (T_{t-\Delta t}), (T_{t-2\Delta t}))$$

(where:  $C_1$  is a constant and  $Q_t$  is the heat flow rate vector at time  $t$ .) This equation may be solved for  $T_t$  since solutions at previous times are known. For more detailed information on the working of ANSYS, the reader is referred to the appropriate manuals: DeSalvo [52] and Kohnke [53].

### 3.3 Verification of ANSYS

Once ANSYS was chosen as the finite element program to be used in the model, it had to be tested and verified. The work selected for comparison was that of Torvik [16] since his finite element model was designed to handle phase change along with temperature distribution. Also, he gives a detailed comparison with known analytical solutions. The third example in his work is the case of the two-dimensional temperature distribution resulting from a steady axi-symmetric flux of a Gaussian distribution acting on a thin sheet. The Gaussian distribution is of the form:

$$F(r) = F \times \exp(-r^2/2\sigma^2)$$

Torvik compares his solutions with the temperature profiles predicted by a computer program written at the Air Force Weapons Laboratory which evaluates the analytical Fourier series solution given by Olcer [54].

A specific case Torvik considers is that of a titanium sheet, 0.0004 m thick and 0.05 m in diameter, initially at 300°K, and having the following thermal properties:

$$\begin{aligned} \rho &= 4430 \text{ kg/m}^3 \\ k &= 14.5 \text{ W/(m}^\circ\text{C)} \end{aligned}$$

$$c_p = 770 \text{ Joules}/(\text{kg}^\circ\text{C})$$

$$T_m = 1900^\circ\text{K}$$

He assumes the disk is subjected to a beam of peak intensity of  $2.0 \times 10^7 \text{ W/m}^2$  with  $\sigma = 0.0025 \text{ m}$ . Torvik uses his model to examine the results of dividing the slab into: a) 10 layers and 40 annular rings using a time step of  $80 \mu\text{sec}$ , and b) 20 layers and 20 annular rings using a time step of  $20 \mu\text{sec}$ . Both cases yielded temperature profiles that differed by less than 1% at a depth of  $2.0 \times 10^{-5} \text{ m}$  for all  $r$  and at times of  $t = 0.03$  and  $0.10 \text{ sec}$ . Also, both cases were in excellent agreement with the Fourier series solution program, especially within the beam radius ( $2\sigma = 0.005 \text{ m}$ ). The exact solution indicated that melting begins at the front surface at  $t = 0.1037 \text{ sec}$ . Torvik's finite element solutions gave  $0.1042$  and  $0.1064 \text{ sec}$ ., respectively.

With these data for comparison, the ANSYS model was set up to establish its accuracy. The Torvik problem was changed only slightly to facilitate later analysis of results using flat plate correlations. Thus, a  $0.05 \text{ m}$  square plate was substituted for the  $0.05 \text{ m}$  radius disk. All other parameters remained the same. Since the present work is concerned only with preventing the plate from starting to melt, the crucial comparison became the exact solution's time of  $t = 0.1037 \text{ sec}$ . (when melting begins at the front surface).

Because the educational version of ANSYS is limited to only a 200 degree of freedom on the wave front, the symmetry of the problem had to be invoked and only the upper right quarter of the plate was modeled. Also, using a technique suggested by Swanson Analysis Systems, Inc., the beam intensity was converted into a convective boundary condition that was applied over the equivalent area of the beam. Borrowing from

Torvik's case b), the equivalent of 20 annular rings was set up--namely, a 20 by 20 element arrangement over the quarter of the plate. This resulted in 400 square elements that were  $1.25 \times 10^{-3}$  m per side covering the quarter of the plate. However, since the educational version of ANSYS could not accommodate 10 layers (much less 20 layers) due to the wave-front limitation, 4 layers had to be selected. The Gaussian distribution of the Torvik problem was handled by taking the radial distance of the center of the face of each element within the beam radius, substituting this distance as  $r$  into the Gaussian distribution equation, and using the resultant intensity value as the average heat transfer coefficient over that element face. Since square elements were being used to approximate a circular beam area, an area 3.45% larger had to be used. The resultant effect was expected to lower the melting initiation time only a slight amount (at most a proportional percentage) due to the fact this extra area was in the edges of the affected area on the plate--the region of lowest intensity because of the beam's Gaussian distribution. For comparison, the model was run under two additional, different conditions: a) the central-most element within the beam radius (in this case the lower-left corner element) was given a convective boundary condition value equal to the peak value of  $2 \times 10^7$  Watts/m<sup>2</sup> (this amounted to an increase of  $1.2 \times 10^6$  Watts/m<sup>2</sup>) which was estimated to give a better approximation due to the nature of the Gaussian distribution; and b) the entire beam area was given a convective boundary condition equal to the peak value in order to note the error incurred by a uniform peak loading.

The results are presented in Table 1 and indicate the ANSYS model is quite acceptable, especially when using the better approximation to

TABLE 1

Test Runs to Establish Accuracy of ANSYS Model<sup>1</sup>

	Time at Initiation of Melting (sec)	% error <sup>2</sup>	Temperature at t = 0.1037 [exact solution] (°K)	% error <sup>3</sup>
1) $1.88 \times 10^7$ W/m <sup>2</sup> on central element <sup>4</sup>	0.1095	+ 5.60%	1829°	- 3.74%
2) $2.0 \times 10^7$ W/m <sup>2</sup> on central element <sup>4</sup>	0.1022	- 1.45%	1919°	+ 1.00%
3) $2.0 \times 10^7$ W/m <sup>2</sup> uniform loading on all elements in affected area	0.0970	- 6.46%	1998°	+ 5.16%

<sup>1</sup> Note: Cases 1) and 2) above use the values noted for the central-most element, and the average values based on radial distance to the center of the face of the element for the other elements within the beam radius.

<sup>2</sup> Note: Percent error is based on comparison to exact solution of t = 0.1037 s for initiation of melting time.

<sup>3</sup> Note: Percent error is based on comparison to the melting point temperature of titanium used by Torvik [16] : 1900°K.

<sup>4</sup> Note: Since the symmetry of the problem is being invoked, only the upper-right quarter of the plate is being examined. Thus, the central element is in actuality the bottom-left corner element on the portion of the plate being examined. Also, this central element represents 1/4 of the central-most actual area of the incident Gaussian laser beam.

the Gaussian distribution (peak intensity for central-most element). Since it was expected that the 3.45% area increase would yield a slightly lower initiation of melting time, the results for the case of  $2 \times 10^7$  Watts/m<sup>2</sup> are especially encouraging and indicate that the ANSYS model is within about 1% of the analytical solution. Also noteworthy is the fact that practically no accuracy was lost due to using 4 layers of elements as opposed to Torvik's 10 and 20 layer arrangements. Of course this result can only be applied with certainty to the case of 0.0004 m thick plates without more testing. However, since the present work is limited to this thickness (except for an example case using aluminum), this finding only further confirms the applicability and accuracy of ANSYS to the portion of the basic problem under consideration. For verification purposes, a copy of one of the computer programs used to test the accuracy of ANSYS is submitted in Appendix A.

### 3.4 Defining Model Parameters

With ANSYS confirmed as appropriate for examining the basic problem, the task undertaken next was defining the limits of the problem. Since ANSYS had just been tested using Torvik's third example, his parameters were retained. Thus, the plate under consideration took on the dimensions of 0.05 m by 0.05 m with a depth of 0.0004 m. For the materials to be studied, titanium was an obvious choice since it had just been tested and since it has many practical applications in the nuclear and laser-machining fields. For comparison, two other widely used materials, aluminum and stainless steel (AISI 304), were also chosen.

Aluminum was selected in order to examine a metal with considerably

different properties than titanium. Aluminum's melting point is nearly 1000°K below that of titanium while its conductivity is approximately an order of magnitude greater. Stainless steel, on the other hand, was selected because its properties fell in between those of titanium and aluminum--although they were more on the order of titanium.

With the dimensions and materials of the plate established, the heating conditions were next. Since  $2 \times 10^7 \text{ W/m}^2$  had just been tested, it was chosen as the base value of intensity. Since Table 1 indicated a +5.16% error in temperature was obtained when using a uniform loading of peak intensity, uniform loading was chosen to insure a safety factor as well as determine an upper bound. Torvik's beam radius (0.005 m) was retained as a base value so that the initial affected area for the quarter of the plate consisted of 13 elements [total area =  $4 \times 13 \times (1.25 \times 10^{-3} \text{ m})^2 = 8.125 \times 10^{-5} \text{ m}^2$ ]. In order to examine the effects of area and intensity on cooling requirements, the intensity was chosen to vary from  $1 \times 10^7 \text{ W/m}^2$  to  $6 \times 10^7 \text{ W/m}^2$  in steps of  $1 \times 10^7 \text{ W/m}^2$ . Affected area was also varied from approximately 30.8% of the original area ( $2.5 \times 10^{-5} \text{ m}^2$ ) to 400% ( $3.25 \times 10^{-4} \text{ m}^2$ )--500% ( $4.0625 \times 10^{-4} \text{ m}^2$ ) for aluminum--with the combined results being presented in tabular and graphical form.

For the cooling part of the problem, liquid sodium, air, and water were chosen as the coolants. Liquid sodium was selected due to its low Prandtl number and air was selected as a representative gas. It was desired to also choose a fluid of high Prandtl number, but at the average temperatures the model deals with (600-950°K), all high Prandtl number fluids the author could identify decomposed. Thus, liquid water at high temperatures and pressures was chosen in order to examine at

least one case of relatively high Prandtl number ( $Pr = 12.0$ ).

To further establish upper-bound conditions, all cooling effects on the surface where the heat source was located were neglected as well as any losses out the plate edges. Also, the model examined only the steady-state condition so as to provide an upper-bound temperature distribution. (Note: For those cases where the steady-state is not an upper bound, the intensity of the heat source will be so great that melting will occur regardless of cooling conditions. Torvik's first example [16] demonstrates this by showing that a finite slab can be considered as being of infinite thickness for very short initial time periods--0.06 seconds for his example.) The rationale behind the above assumptions was that if cooling conditions could be established that would prevent melting under these upper-bound conditions, then these cooling conditions should offer a margin of safety under actual conditions as well as reliable minimum cooling requirements.

Thus, with all these factors incorporated, the final product of the model becomes a heat transfer coefficient that will prevent melting under upper-bound conditions. This heat transfer coefficient is then used along with local Nusselt number correlations for a vertical flat plate to determine if cooling is possible under free or forced convection and, if cooling is indeed possible, under what specific conditions. A copy of a sample program used in determining these conditions is submitted in Appendix B. The results of the model's computations are presented and discussed in the next chapter.

## Chapter 4

### NUMERICAL SOLUTIONS AND CORRELATION RESULTS

#### 4.1 Presentation of Numerical Solutions

In order to obtain the desired solutions, the author had to function as an optimizer for the ANSYS program--supplying estimates of the appropriate heat transfer coefficient to the program and then altering the value after the program had returned an appropriate temperature distribution. (Swanson Analysis Systems, Inc., just recently added an optimizer module to ANSYS. Unfortunately, it was not available during the execution of this work.) Since the average run took about 40 minutes of CPU time (and up to three hours of connect time), the process proved to be extremely time consuming. Fortunately, the author was given four different computer accounts and this expedited matters somewhat. Even so, the above time constraints forced some interpolation of values that the author would have preferred to forgo, however these are noted where they occur and are estimated to be well under 1% in error. Summaries of the results are presented below.

##### 4.1.1 Heat Transfer Coefficient as a Function of Heat Source Intensity

Figure 1 is a combined graph of the response of all three metals to the range of intensities ( $1 - 6 \times 10^7 \text{ W/m}^2$ ) under study. The initial response is as intuitively expected, with the metals having the highest conductivities requiring the most cooling. The approximate linearity of the aluminum response can be partly explained by its high conductivity (at least an order of magnitude greater than titanium and stainless steel) and partly explained by the fact its conductivity is decreasing with temperature. The similarity of the stainless steel and titanium

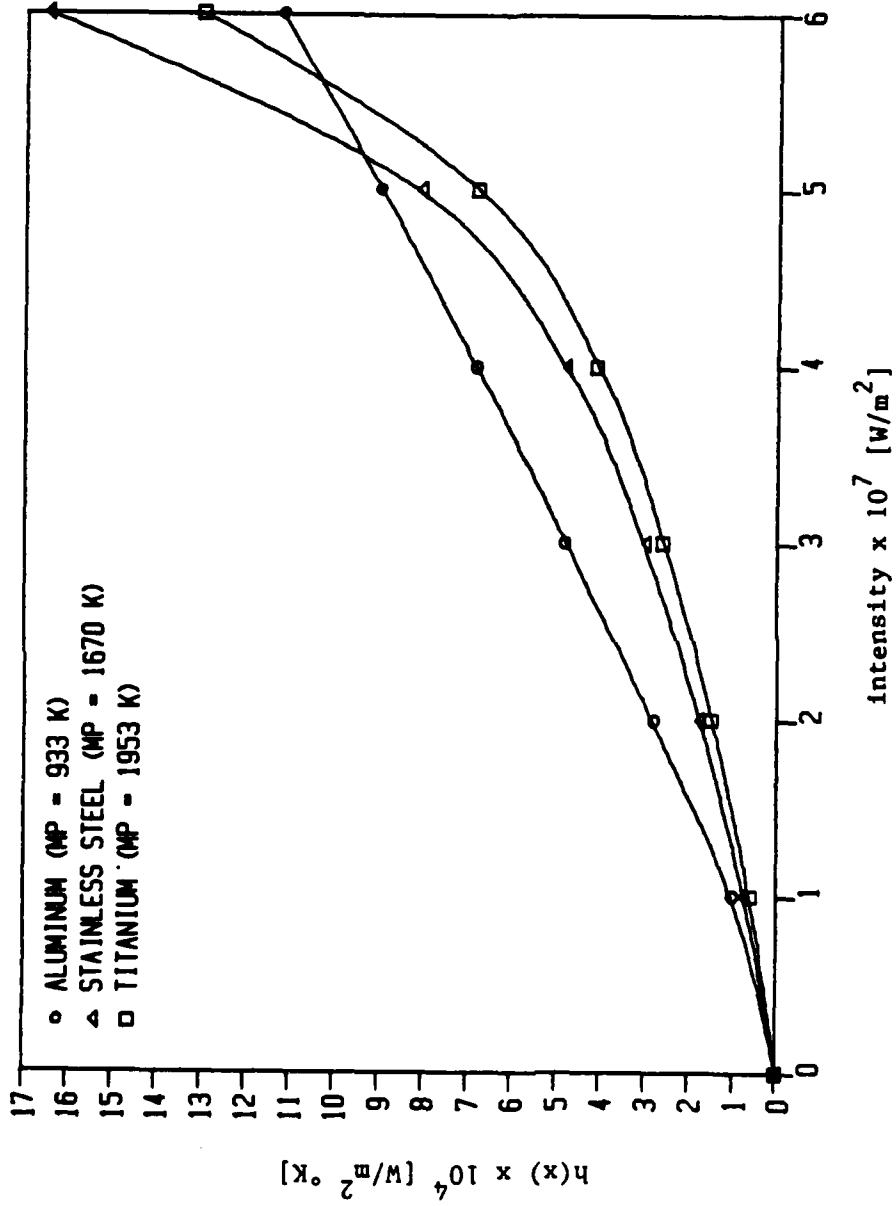


Figure 1. Minimum heat transfer coefficient  $[h(x)]$  plotted as a function of localized heat source intensity for aluminum, stainless steel, and titanium plates, 0.0004 m thick.

responses are expected since their conductivities are approximately the same and also increase with temperature.

To fully understand Figure 1, especially the aluminum response curve's crossing of the titanium and stainless steel response curves between  $5 - 6 \times 10^7 \text{ W/m}^2$ , an examination of the basic governing equations is necessary. The heat flux ( $q_x$ ) through the plate is approximately defined by a simplified form of Fourier's law to be:

$$q_x = k(T_F - T_B)/L$$

where:  $k$  is the conductivity;  $T_F$  is the temperature on the front face of the plate (the side with the heat source);  $T_B$  is the temperature on the back face of the plate (the side with the coolant); and  $L$  is the thickness of the plate.

For the convection process on the back of the plate, Newton's law of cooling defines the heat flux from the plate (in this case,  $q_x$ ) to be:

$$q_x = h(T_B - T_\infty)$$

where:  $h$  is the heat transfer coefficient,  $T_B$  is the temperature of the back face of the plate; and  $T_\infty$  is the fluid free stream temperature.

Combining and rearranging the above two relations to obtain an expression for  $h$  yields:

$$h = k(T_F - T_B)/L(T_B - T_\infty)$$

For the case of each metal in the present work:  $T_F$ ,  $L$  and  $T$  are all constant. The conductivity ( $k$ ) varies with temperature through the plate for all three metals, but since  $k$  is so large for aluminum, the temperature difference through the aluminum plate is relatively constant (varying from  $33^\circ$  to about  $100^\circ$ ) for all intensities. This explains the resulting near-linear behavior.

On the other hand, for the case of titanium and stainless steel, not only does  $k$  increase with temperature (and thus intensity of heat source), but  $T_B$  decreases dramatically with increase of intensity. For example, the temperatures on the back face of titanium and stainless steel are approximately 1600°K and 1400°K, respectively, for the  $2 \times 10^7$  W/m<sup>2</sup> intensity. For  $6 \times 10^7$  W/m<sup>2</sup>, the temperatures have dropped to 762.5°K and 665°K respectively. Thus, not only is the denominator decreased, but the numerator is markedly increased too, so that the value of  $h$  increases almost exponentially. This behavior can be attributed to the relatively poor conductivity of stainless steel and titanium as compared to aluminum. Thus, for stainless steel and titanium to keep from melting as the intensity increases, a large temperature gradient must be created by almost exponential increases of heat transfer by convection. Therefore, once examined in detail, the crossing of the response curves is expected.

Note must also be made of why  $6 \times 10^7$  W/m<sup>2</sup> was determined as the maximum intensity to be examined. Since the present work is concerned with only free and forced convection cooling, exceeding  $6 \times 10^7$  W/m<sup>2</sup> would definitely produce heat transfer coefficients outside of those cooling regimes. According to Incropera and DeWitt (55), typical values of heat transfer coefficient for forced convection using liquids range from 50 - 20,000 W/m<sup>2</sup>°K while boiling values range up to 100,000 W/m<sup>2</sup>°K. Since the model produces heat transfer coefficients in excess of 100,000 W/m<sup>2</sup>°K for a heat intensity of  $6 \times 10^7$  W/m<sup>2</sup> this intensity is easily an upper bound for the present work.

A listing of the model generated data for Figure 1 appears in Appendix C. Conductivity values are confirmed in Incropera and Dewitt

[55] and Touloukian and Ho [56].

#### 4.1.2 Heat Transfer Coefficient as a Function of Affected Area at Various Intensities

Figures 2-4 show the combined relations between heat transfer coefficient as a function of affected area at various intensities ranging from  $1 - 6 \times 10^7 \text{ W/m}^2$ . The  $2 \times 10^7 \text{ W/m}^2$  intensity line is the base line in each graph since it has the most complete set of data for each material. Data points for all  $2 \times 10^7 \text{ W/m}^2$  lines are plotted as triangles. Squares mark the value of other data points that were actually computed by the model either by exact calculation or interpolation/extrapolation of model generated values. The data from Figure 1 is also included and plotted as squares.

All graphs behave similar--with a fairly rapid rise as the affected area first begins to grow to an almost just as rapid leveling-off (after a certain "critical" area) beyond which increase of area has relatively little effect on heat transfer coefficient. The apparent "critical" area is reached earlier with lower conductivity values, probably because the conditions that approximate the case of a constant heat flux over the entire surface are arrived at sooner. This is probably the reason for the fairly rapid leveling-off behavior too since, as the area affected by the heat source increases, the problem begins to locally take on the appearance of a wall over which its entire surface is subjected to a constant heat flux. From a local perspective with respect to the plate, the case of constant heat flux is exactly what is transpiring, and so a nearly constant value of heat transfer coefficient is to be expected.

Another interesting trend shown on the charts is found in the

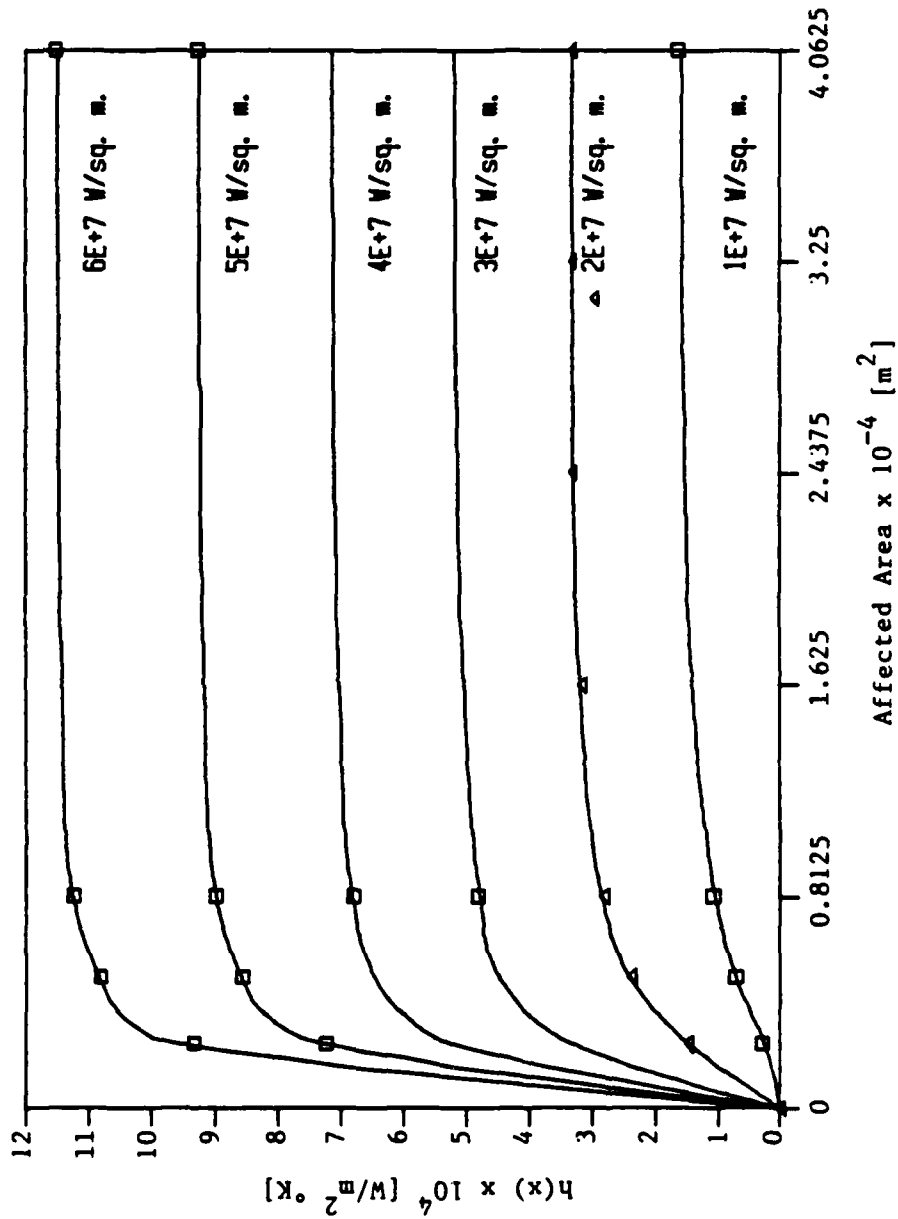


Figure 2. Minimum heat transfer coefficients for aluminum plotted as functions of area affected by a localized high intensity heat source at intensities of  $1 - 6 \times 10^7$  W/m<sup>2</sup>. Plotted points (squares and triangles) are actual model generated data.

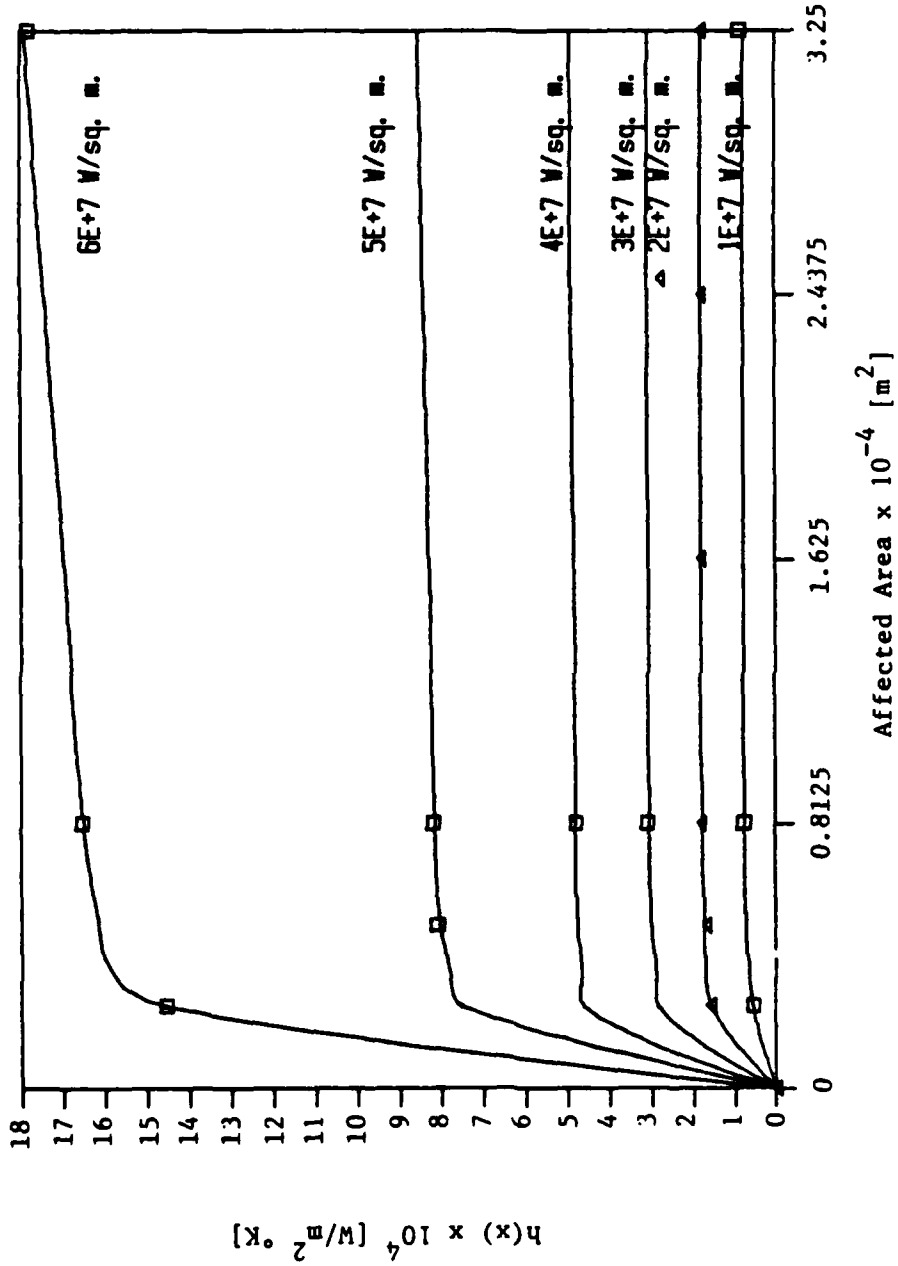


Figure 3. Minimum heat transfer coefficients for stainless steel plotted as functions of area affected by a localized high intensity heat source at intensities of  $1 - 6 \times 10^7 \text{ W/m}^2$ . Plotted points (squares and triangles) are actual model generated data.

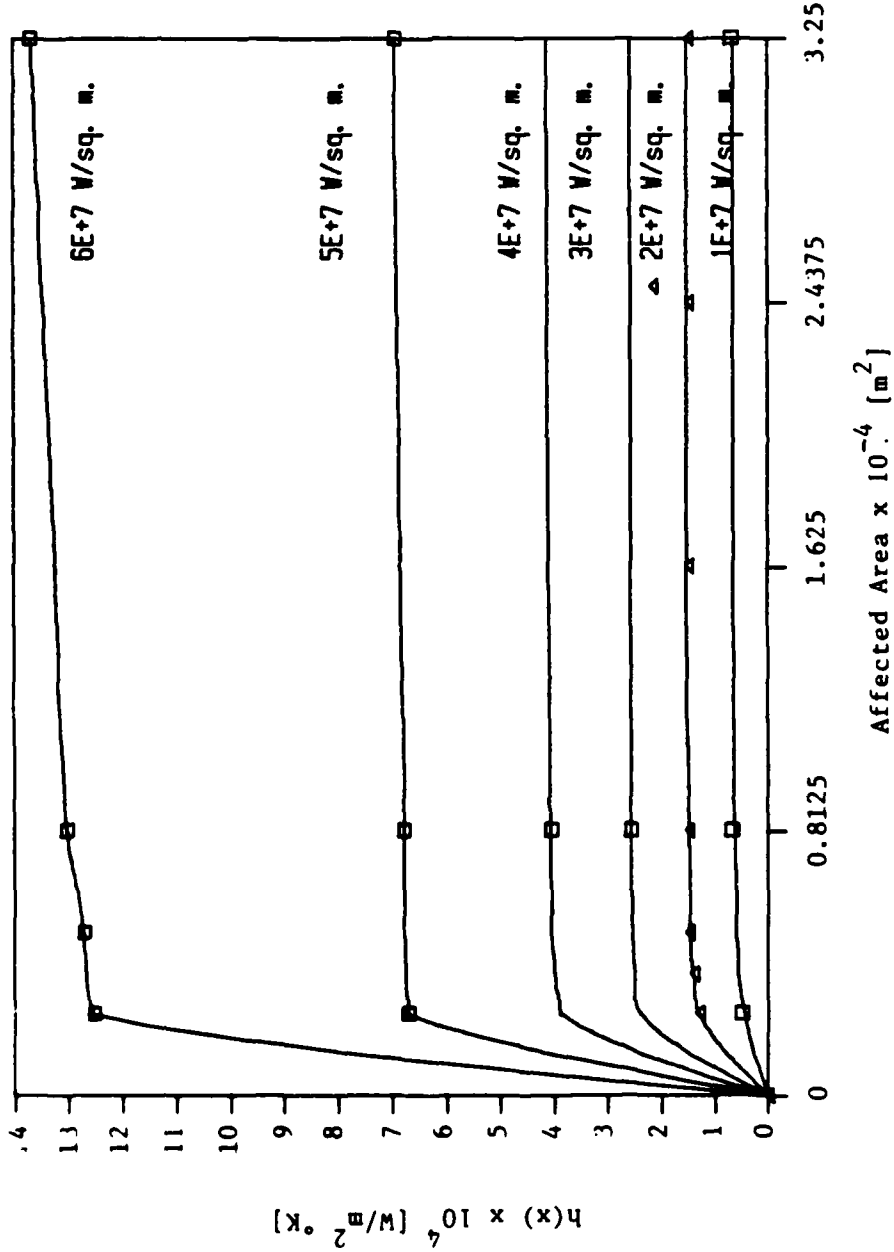


Figure 4. Minimum heat transfer coefficients for titanium plotted as functions of area affected by a localized high intensity heat source at intensities of  $1 - 6 \times 10^7$  W/m<sup>2</sup>. Plotted points (squares and triangles) are actual model generated data.

graphing of the study's intensity range ( $1 - 6 \times 10^7 \text{ W/m}^2$ ) values. In the case of stainless steel and titanium, with their relatively low heat conductivities that increase with temperature, an ever-increasing spacing is noted as intensity increases. For aluminum, with its relatively high conductivity that decreases with temperature, the spacing is approximately equal. In light of Figure 1, this graphical result was expected.

In addition to these values, the model calculated some key points that are also plotted as squares on the graph in order to predict the shapes of the rest of the curves. Some of the values are generated by the model exactly while others are interpolated/extrapolated from model data. Data points used are tabulated in Appendix D with interpolations and extrapolations noted.

#### 4.1.3. Heat Transfer Coefficient as a Function of Thickness in Aluminum

During the course of the present work, it was discovered that because of aluminum's high conductivity, the 4-layer element arrangement could be replaced by just one layer with a change of only about  $0.1^\circ\text{K}$ . In fact, it was learned that the single element's depth could be extended to  $0.0008 \text{ m}$  with less than a  $0.2^\circ\text{K}$  change. This discovery not only cut down the run time of the aluminum jobs to about 25% of the original time, but also allowed the examination of aluminum plates up to  $0.0032 \text{ m}$  thick while maintaining essentially the same accuracy (within  $0.02\%$ ). The graph showing the findings is presented in Figure 5, while tabulated data is submitted in Appendix E. The best-fit curve presented is a regression polynomial of order 2. The one data point denoted by a square is the theoretical value of the heat transfer coefficient for the

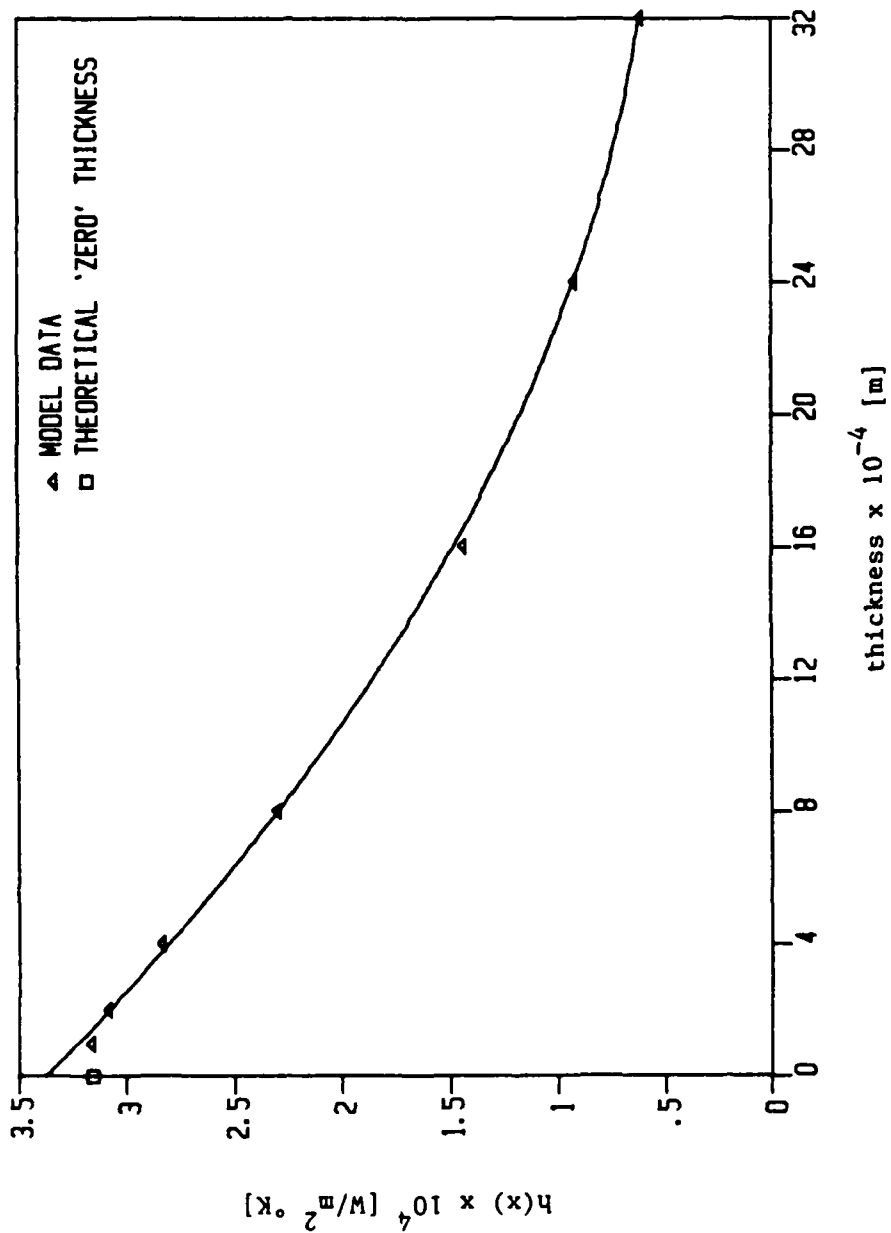


Figure 5. Minimum heat transfer coefficient  $[h(x)]$  required for cooling an aluminum plate plotted as a function of thickness of the plate. The heat source is  $2 \times 10^7 \text{ W/m}^2$ , localized to a  $0.005 \text{ m}$  radius in the center of the plate.

case of a plate with 'zero' thickness (i.e. 100% heat conduction). The extrapolated value of the best-fit curve with the y-axis yields a value of about  $3.38 \times 10^4 \text{ W/m}^2\text{K}$ --or less than 7.0% high. The difference can be explained by the fact that the idealization of using the average of the plate temperature and the fluid free stream temperature to determine coolant properties will generally yield local temperatures lower than in the actual case. Still, the curve behaves as expected, with the heat transfer coefficient decreasing with increased plate thickness.

#### 4.1.4 Heat Transfer Coefficient Versus Conductivity

A bar graph of the minimum heat transfer coefficients for the various metals versus each metal's conductivity is presented in Figure 6. The values are those which result from the base intensity of  $2 \times 10^7 \text{ W/m}^2$ . Only three model-generated data points are available at this intensity since only three materials were studied. Further study of more materials is required to establish possible trends. The data for this graph is submitted in Appendix F.

#### 4.2 Nusselt Number Correlations for Free and Forced Convection

Given the heat transfer coefficients needed to prevent melting, it was now necessary to translate them into suggested cooling conditions. To do this, Nusselt number correlations were required since the Nusselt number provides a measure of the convection heat transfer occurring at the surface of the plate. Thus, Nusselt number correlations were needed for a vertical flat plate under both free and forced convection conditions. Even though according to Incropera and DeWitt [55] the heat transfer coefficients produced by the model were in the upper range of

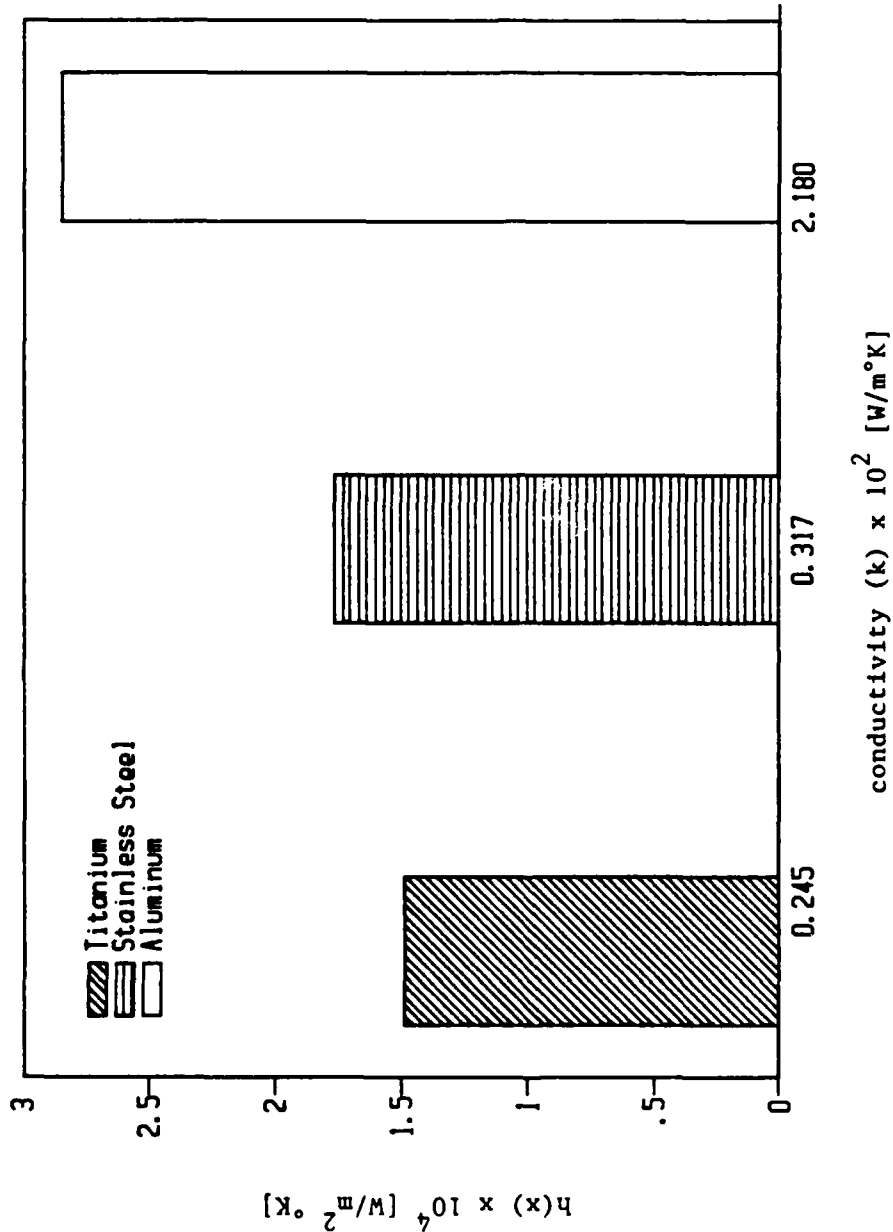


Figure 6. Minimum heat transfer coefficient versus each metal's conductivity (titanium, stainless steel, and aluminum) for the case of heat intensity =  $2 \times 10^7$  W/m<sup>2</sup>.

typical forced convection values for liquids, the free convection correlations were still investigated mainly for the purpose of examining the case of liquid sodium for future study. The literature was searched for correlations that would cover the low-to-high Prandtl number range as well as the laminar and turbulent regimes of free and forced convection. The correlations that were used are presented below along with further references.

#### 4.2.1 Nusselt Number Correlations for Free Convection

Most of the work done in free convection correlations deals with either a constant temperature or constant heat flux situation. Both laminar and turbulent flows have been examined. Under laminar flow conditions Kays and Crawford [57] state the constant heat flux case yields Nusselt numbers about 15% higher than the constant temperature case while in turbulent flow both cases yield similar Nusselt numbers. Since the present work is concerned with examining minimum cooling requirements for upper bounds, the constant temperature correlations were chosen. Therefore, if cooling conditions could be established that prevented melting under constant temperature conditions, constant heat flux conditions would be satisfied too. Of course, the present work's situation is more like that of an "unheated starting length" problem, but considering the complete plate to be at constant temperature provides a further upper bound to the problem.

For readers interested in the constant heat flux case, Fujii and Fujii [58] and Churchill and Ozoe [59] examine the laminar flow regime. Turbulent flow free convection is examined by Vliet and Ross [60] and Vliet and Liu [61]. Though the above listings are obviously not

comprehensive, they will give the interested reader an idea of what work has been done in the field.

Nusselt number correlations for free convection are usually functions of the Prandtl number and Grashof number. The Prandtl number of a fluid provides a measure of the relative effectiveness of momentum transfer by diffusion compared to energy transfer by diffusion. The Prandtl number is fixed by properties of the fluid ( $\nu$ : kinematic viscosity and  $\alpha$ : thermal diffusivity) and thus provides no latitude in adjusting the Nusselt number. The Grashof number provides a measure of the ratio of buoyancy forces to viscous forces in the velocity boundary layer. It too is largely fixed by properties of the fluid ( $\beta$ : volumetric thermal expansion coefficient and  $\nu$ ) as well as temperature conditions of the problem. Thus, as expected, when dealing with a free convection situation the main way to adjust the Nusselt number is to change the cooling fluid. So in examining cooling problems involving free convection, the main question is whether the cooling requirements can be met with the fluids available. The correlations found to answer that question immediately follow.

#### 4.2.1.1 Free Convection--Laminar Flow--Constant Temperature

Since the present work uses liquid sodium, air, and water as the potential coolants, correlations were needed for Prandtl numbers in the range from approximately 0.005 to 12.0. For the case of the lower end of this range, LeFevre [62] determined limiting correlations as Prandtl number approaches 0 and infinity. For the present work, his correlation for the lower limit was used to examine the case of liquid sodium:

$$Nu(x) = 0.600(Gr(x)Pr^2)^{0.25}$$

For the case of air ( $Pr = 0.7$ ), the correlation developed by Churchill and Usagi [63] was used:

$$Nu(x) = 0.503Gr(x)^{1/4}Pr^{1/4}/[1 + (0.492/Pr)^{9/16}]^{4/9}$$

For the case of water ( $Pr = 1.0$  and  $12.0$ ), the expression reported by Ede [64] was used:

$$Nu(x) = 0.75[2Pr/5(1 + 2Pr^{1/2} + 2Pr)]^{1/4} [Gr(x)Pr]^{1/4}$$

#### 4.2.1.2 Free Convection--Turbulent Flow--Constant Temperature

As with laminar flow, correlations applicable over the same Prandtl number range were needed. For the cases of liquid sodium ( $Pr = 0.005$ ) and air ( $Pr = 0.7$ ), the work of Bailey [65] was employed. For sodium, the correlation used was:

$$Nu(x) = 0.060Gr(x)^{1/4}$$

The above correlation applies for the Grashof number range:  
 $10^{10} - 10^{15}$ .

For air, Bailey found the following applied:

$$Nu(x) = 0.183(Gr(x)Pr)^{0.31}$$

This relation is valid for air in the Grashof number range:  
 $10^9 - 10^{15}$ .

For the case of water ( $Pr = 1.0$ ), the work of Eckert and Jackson [66] was used. They found the following applied for  $Pr = 1.0$  and  $Gr(x) = 10^{10} - 10^{12}$ :

$$Nu(x) = 0.0295[Pr^7/(1 + 0.49Pr^{2/3})^6]^{1/15}Gr(x)^{2/5}$$

The reason the ranges of Grashof number in the turbulent flow regime usually have a lower limit of about  $Gr(x) = 10^{10}$  is because it is around this value that turbulent free convection is realized. Pitts and Sissom [67] state that the transition from laminar to turbulent flow in natural

(free) convection usually occurs when the product of Prandtl number and Grashof number equals approximately  $10^9$ .

For other work in the area of free convection, see the references at the end of this work [68-71].

#### 4.2.2 Nusselt Number Correlations for Forced Convection

As with free convection, much of the work accomplished dealing with forced convection over flat plates is concerned with either the constant temperature case or the constant heat flux case. Since Kays and Crawford [57] state that constant heat flux correlations yield Nusselt numbers approximately 36% higher in laminar flow and about 4% higher in turbulent flow than their constant temperature counterparts, the constant temperature correlations will again be the ones used. (For the constant heat flux case, Kays and Crawford [57] also give a summary of the correlations available as well as the work done in the field). Also, like free convection, the "unheated starting length" problem is being treated as a constant temperature condition over the entire plate in order to establish an upper bound to the problem of minimum cooling requirement determination.

For the forced convection correlations, Nusselt numbers are expressed as functions of Prandtl number and Reynolds number. The Reynolds number provides a ratio of inertia to viscous forces. Unlike its counterpart in free convection (the Grashof number), the Reynolds number can be used to adjust the Nusselt number without having to change cooling fluids. This adjustment can be made by increasing the free stream velocity of the fluid passing over the plate. Thus, for the present study, the objective of using the forced convection correlations

will be to determine a velocity necessary so that the cooling fluid in question will meet the minimum cooling requirements. If the velocity determined is unattainable by normal processes used today, the cooling fluid will be deemed "disqualified". A summary of the correlations used in the present work follows.

#### 4.2.2.1 Forced Convection--Laminar Flow--Constant Temperature

Kays and Crawford [57] present Nusselt number correlations valid for very low to very high Prandtl numbers. Their correlations are used in the present work for the cases of air and water. For moderate values of Prandtl number ( $Pr = 0.5 - 10.0$ ), they present the following correlation:

$$Nu(x) = 0.332Pr^{1/3}Re(x)^{1/2}$$

(This correlation is also reported by Incropera and DeWitt [55].)

For very high Prandtl numbers ( $Pr > 10.0$ ), the above correlation is slightly modified to:

$$Nu(x) = 0.339Pr^{1/3}Re(x)^{1/2}$$

For the very low Prandtl number case, Eckert and Drake [72] give a correlation valid for the range:  $0.005 < Pr < 0.05$ . The correlation used was:

$$Nu(x) = [Re(x)Pr]^{1/2} / [1.55Pr^{1/2} + 3.09(0.372 - 0.15Pr)^{1/2}]$$

Thus, this correlation was used for examining liquid sodium as a coolant.

It is important to note that laminar flow over a flat plate has a limiting Reynolds number of approximately 60,000. After this critical Reynolds number is reached, the flow begins to transition to the turbulent regime.

#### 4.2.2.2 Forced Convection--Turbulent Flow--Constant Temperature

For the moderate Prandtl number range ( $0.5 < Pr < 5.0$ ), valid for air and for water under high pressure, Kays and Crawford [57] give a correlation good for Reynolds numbers up to several million:

$$Nu(x) = 0.0287PrRe(x)^{0.8} / [0.169Re(x)^{-0.1}(13.2Pr - 10.16) + 0.9]$$

For the case of water under very high pressure ( $Pr = 12.0$ ) and the case of liquid sodium ( $Pr = 0.005$ ), Eckert and Drake [73] give the following correlation valid for Reynolds numbers up to  $10^7$  :

$$Nu(x) = 0.0296PrRe(x)^{0.8} / [1 + 0.87A(Re(x))^{-0.1}(Pr-1)]$$

where:

$$A = 1.5Pr^{-1/6}$$

#### 4.3 Cooling Condition Determination and Coolant Evaluation Results

With the above Nusselt number correlations, minimum cooling conditions can be established and coolant suitability can be evaluated. In evaluating the minimum cooling conditions, a minimum Nusselt number must be established for each individual case. Thus, if cooling conditions can be designed that exceed this minimum Nusselt number, melting of the metal plates will be prevented. To establish this minimum local Nusselt number, the definition of Nusselt number is invoked. Namely:

$$Nu(x) = h(x)x/k_f$$

The  $h(x)$  value is supplied by the model and is the heat transfer coefficient that will prevent any melting of the plate. The distance  $x$  in the present work is 0.025 m (the center of the plate), since this is the location of the highest temperature on the back face (as well as the

front face) of the plate.

The conductivity of the fluid is  $k_f$  and is evaluated at the average temperature between the backside of the plate and the free stream temperature. The backside temperature of the plate is supplied by the model while the free stream temperature is defined to be 300°K. The resulting minimum local Nusselt numbers are given in Table 2. (Note: The special cases where water under high pressure is the coolant were included for the express purpose of examining a fluid with Prandtl numbers of 1.0 and 12.0.)

Once the minimum cooling requirements were established for each metal/coolant combination, the Nusselt number correlations could be graphed to determine the suitability of the coolants under forced and free convection conditions. Figures 7 - 12 show the results for forced convection correlations. On these graphs, intersection of the minimum local Nusselt number lines with the correlation lines yield minimum Reynolds numbers necessary to prevent melting. For free convection correlations, Figures 13 and 14 show the results. On these graphs, intersection of the minimum local Nusselt number lines with the correlation lines yield minimum Grashof numbers necessary to prevent melting.

#### 4.3.1 Forced Convection Results

One fact is readily apparent upon examining Figures 7 - 12; namely, the laminar flow regime is totally disqualified as a possible cooling condition. This is not really a surprise since the problem does involve a high intensity heat source and since the heat transfer coefficients calculated by the model were definitely in the upper range of typical

TABLE 2

## Minimum Local Nusselt Numbers

[ 0.05 m Square Plate, 0.0004 m thickness,  $2 \times 10^7$  W/m<sup>2</sup> Heat Source ]

Metal/Coolant	Prandtl Number	Average Temperature ( $T_B + 300$ )/2	Conductivity of Coolant ( $k_f$ : W/m <sup>2</sup> K)	Minimum Nusselt # [ $h(x)0.025/k_f$ ]
Aluminum/ Sodium	0.005	600°K	76.40	9.326
Stainless Steel/ Sodium	0.005	850°	64.65	6.845
Titanium/ Sodium	0.005	950°	60.40	6.167
Aluminum/ Air	0.7	600°	0.0469	15191.9
Stainless Steel/ Air	0.7	850°	0.0596	7424.5
Titanium/ Air	0.7	950°	0.0643	5793.2
Aluminum/ H <sub>2</sub> O*	1.0	600°	0.497	1433.6
Titanium**/ H <sub>2</sub> O***	12.0	645°	0.331	5113.3

\* H<sub>2</sub>O under pressure of  $1.235 \times 10^7$  W/m<sup>2</sup>\*\* Heat Source (for this case only) =  $5 \times 10^7$  W/m<sup>2</sup>\*\*\* H<sub>2</sub>O under pressure of  $2.152 \times 10^7$  N/m<sup>2</sup>

values for forced convection liquid cooling (according to Incropera and DeWitt [55]). To determine the velocities necessary for each coolant, each graph must be examined separately.

To demonstrate how the following graphs were constructed, the steps taken to produce Figure 9 (the sodium coolant evaluation) are displayed in Figures 7-8. In Figure 7, the minimum local Nusselt number lines for each of the three metals under construction are plotted. In Figure 8, the laminar and turbulent Nusselt number correlations are graphed for forced convection conditions involving fluids with Prandtl numbers between 0.005 and 0.05. Figures 7 and 8 are then combined to form Figure 9.

In Figure 9, the turbulent correlation line intersects the minimum Nusselt number lines for titanium and aluminum at Reynolds number values of 30,000 and 68,000 respectively (titanium and aluminum are analyzed to establish a range of applicable velocities). Rearranging the defining expression for local Reynolds number yields an expression for calculating free-stream velocity:

$$u_{fs} = Re(x)v/x$$

Since  $x$  equals the local distance in question (the center of the plate, 0.025 m) and  $v$  equals the kinematic viscosity at the average temperatures (approximately  $4.0 \times 10^{-7} \text{ m}^2/\text{s}$  [aluminum] and  $2.35 \times 10^{-7} \text{ m}^2/\text{s}$  [titanium]), the appropriate free stream velocity can be calculated. The result is a free stream velocity of approximately 0.28 m/s for titanium and 1.09 m/s for aluminum. Since these velocities are easily attainable, the conclusion is liquid sodium would serve as a viable coolant for the present situation of a 0.0004 m thick metal plate heated by a  $2 \times 10^7 \text{ W/m}^2$  heat source.

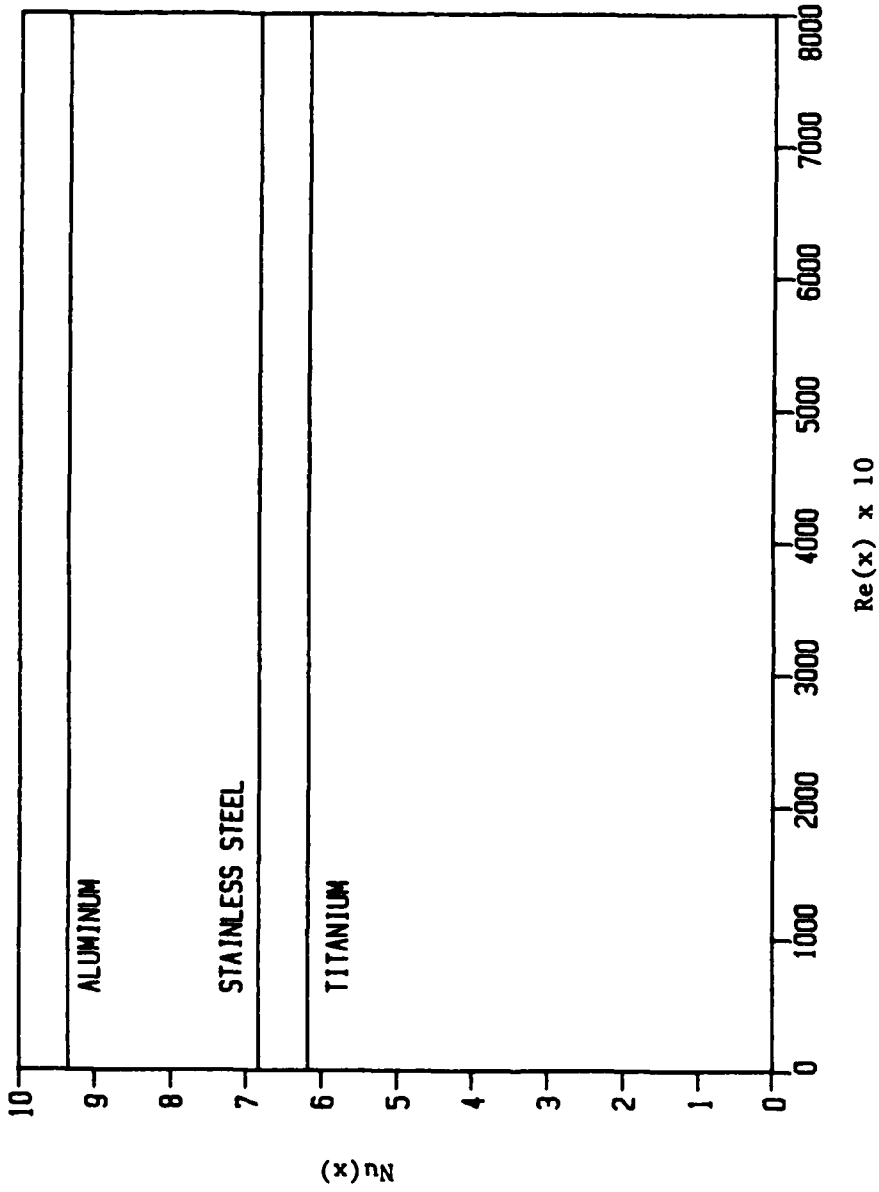


Figure 7. The minimum Nusselt numbers required to prevent melting in each metal plate are plotted versus Reynolds number to demonstrate how the graph is constructed.

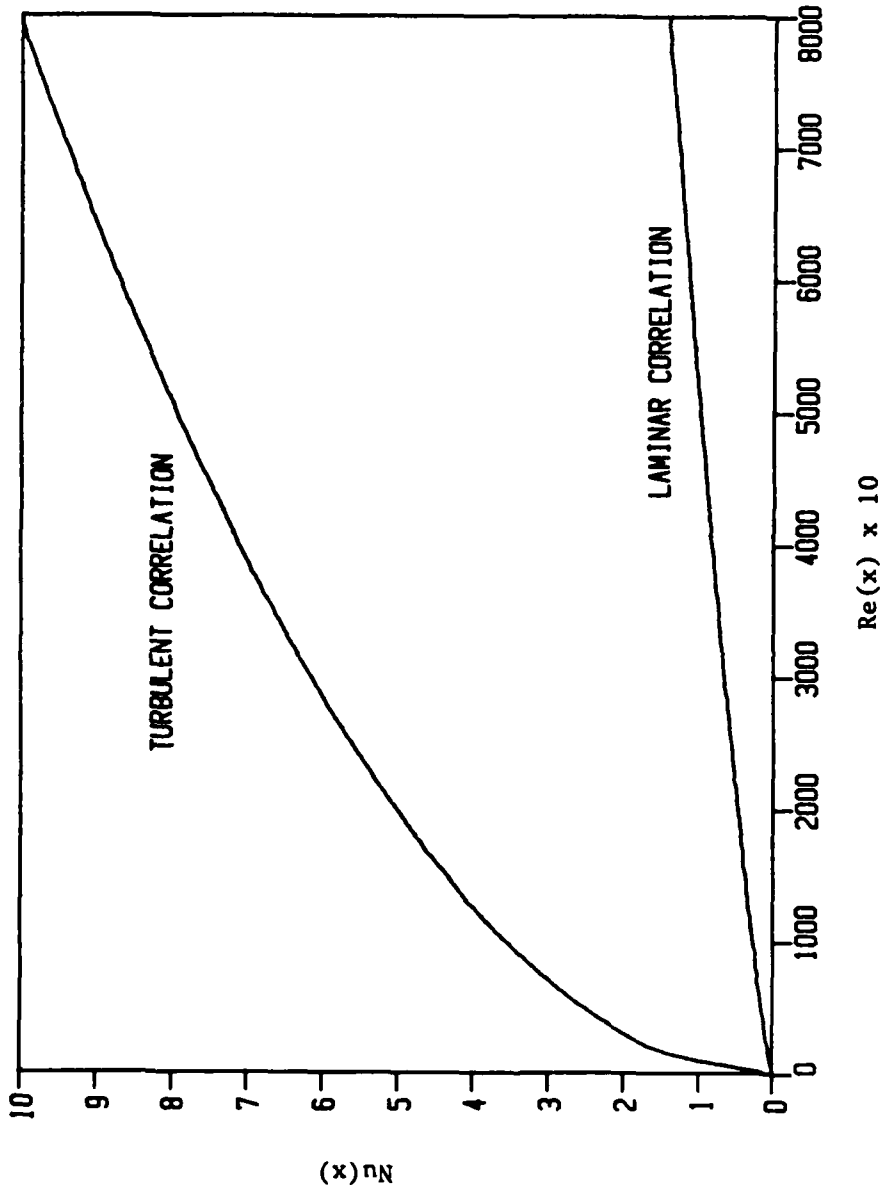


Figure 8. The turbulent and laminar Nusselt number correlations are plotted to demonstrate both the large difference in the correlations as well as the construction of the combined figure.

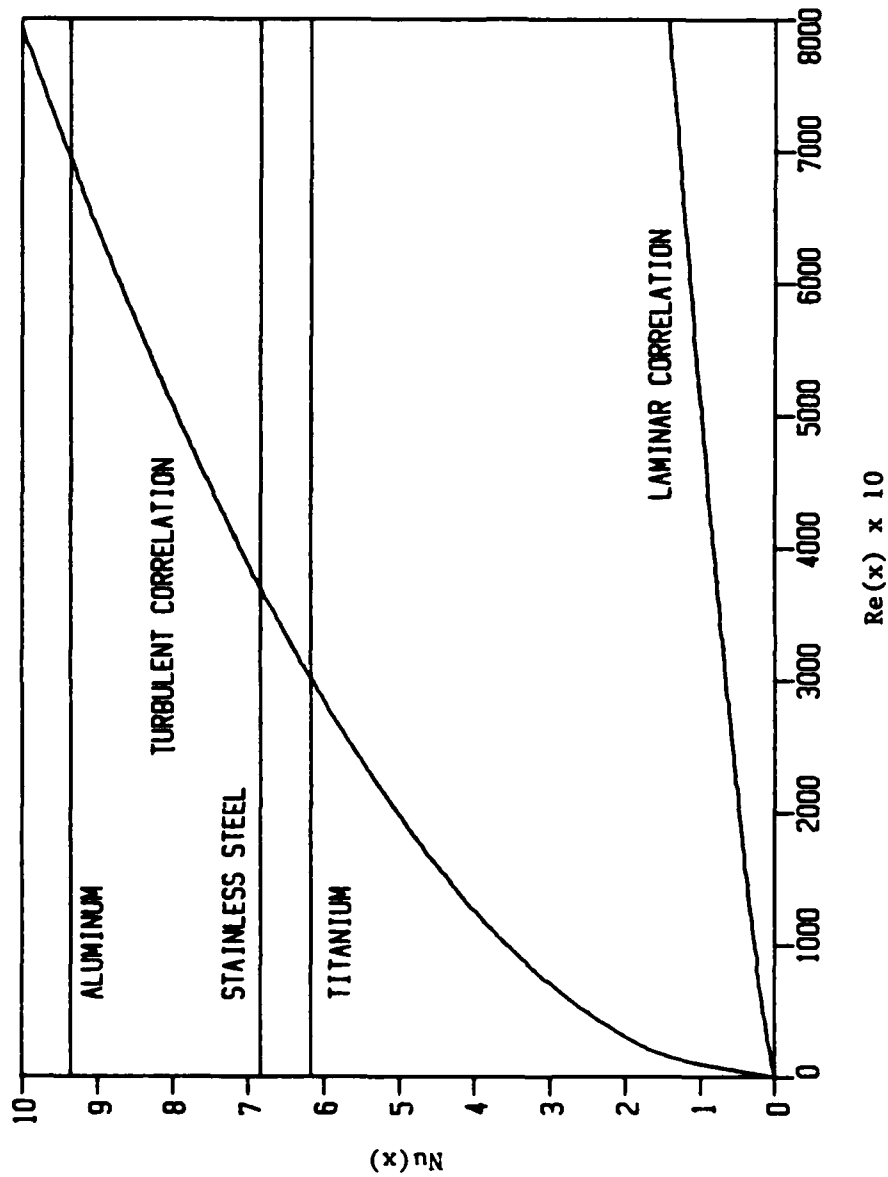


Figure 9. The combined figure for sodium as the coolant results from overlaying Figure 7 on Figure 8. The resulting intersections of the correlations with the minimum Nusselt number lines for the respective metals yield a minimum Reynolds number necessary to prevent melting using sodium as the coolant for each case. (The rest of the figures presented will be combined figures.)

In Figure 10, the necessary Reynolds number is almost two orders of magnitude greater than those in Figure 9. Since the correlation being graphed is only valid for Reynolds numbers of up to several million, evaluating the case for titanium should reveal the feasibility of using air as the coolant. The correlation line intersects the titanium minimum cooling line at approximately a Reynolds number of 5,600,000. The kinematic viscosity of air at 950°K is  $112.2 \times 10^{-6} \text{ m}^2/\text{s}$ . Again using  $x$  as the center of the plate (0.025m), the resulting free stream velocity is approximately 25,133 m/s (or 56,221 mph). Since this velocity is unattainable by normal processes, air is totally disqualified for forced convection cooling.

In examining the special case of aluminum/water (Figure 11), the Reynolds number at the intersection of the minimum cooling line and the Nusselt number correlation is approximately 780,000. Using 0.025 m for  $x$  and  $1.248 \times 10^{-7} \text{ m}^2/\text{s}$  for the kinematic viscosity, the free stream velocity is approximately 3.89 m/s. This result makes water at  $1.235 \times 10^7 \text{ N/m}^2$  a viable coolant for the case of aluminum.

The resulting Reynolds number for the special case of titanium/water (Figure 12) is just somewhat below that of aluminum/water:  $Re(x) = 730,000$ . The conditions of the titanium/water problem, though, are completely different--with a higher heat source intensity of  $5 \times 10^7 \text{ W/m}^2$  and a higher Prandtl number of 12.0. The kinematic viscosity for water at  $2.152 \times 10^7 \text{ N/m}^2$  is  $1.270 \times 10^{-7} \text{ m}^2/\text{s}$ . Using 0.025 m for  $x$  yields a free stream velocity of 3.71 m/s. Thus, water at  $2.152 \times 10^7 \text{ N/m}^2$  is a viable cooling option for the case of titanium subjected to a  $5 \times 10^7 \text{ W/m}^2$  heat source. Of course, the capability to put the water under a pressure of  $2.152 \times 10^7 \text{ N/m}^2$  must

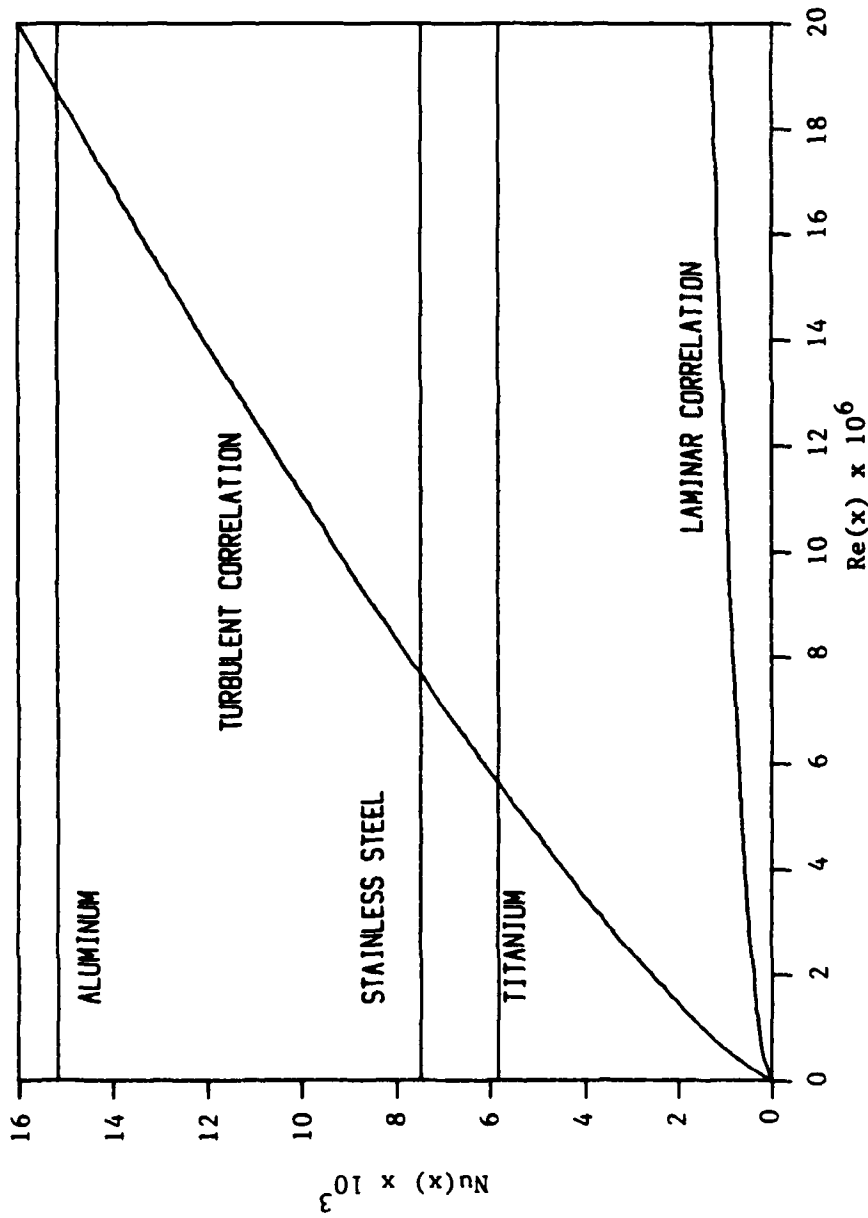


Figure 10. The combined minimum Nusselt numbers and turbulent and laminar Nusselt number correlations for air. Intersections yield Reynolds numbers much too high to be practical.

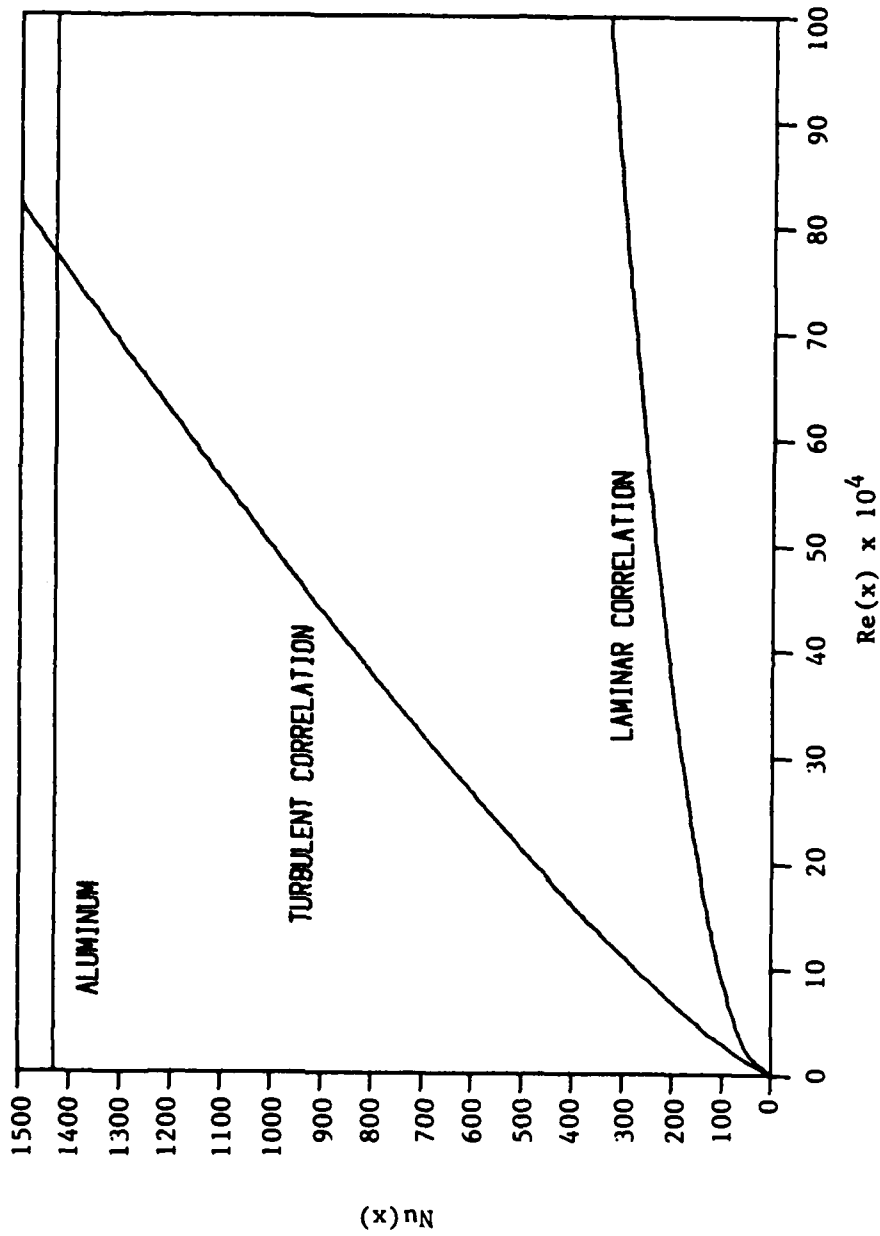


Figure 11. The special case of water under high pressure ( $1.235 \times 10^7 \text{ N/m}^2$  and  $Pr = 1.0$ ) cooling aluminum subjected to a  $2 \times 10^7 \text{ W/m}^2$  localized heat source. The minimum Nusselt line for aluminum intersects the turbulent Nusselt number correlation at a Reynolds number of about 780,000.

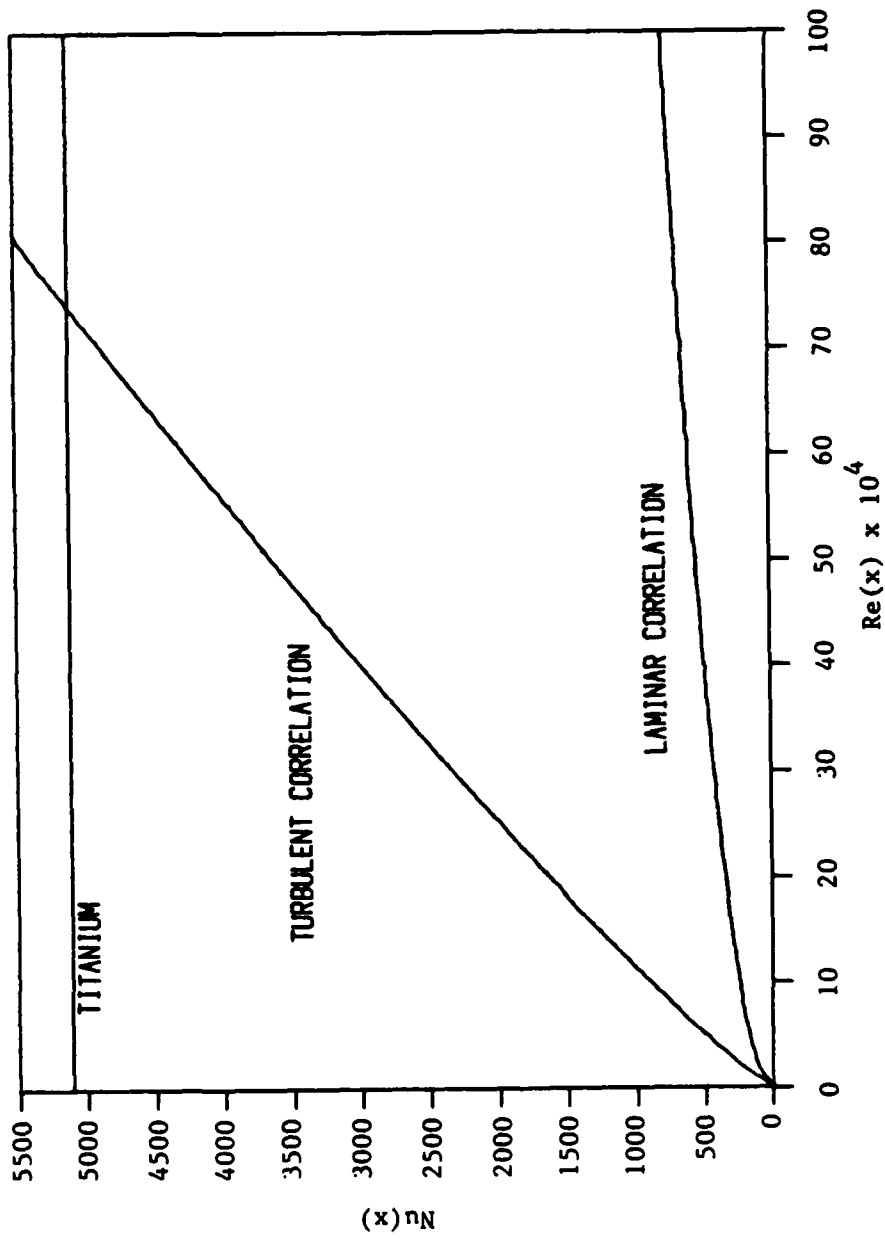


Figure 12. The special case of water under very high pressure ( $2.152 \times 10^7 \text{ N/m}^2$  and  $Pr = 12.0$ ) cooling titanium subjected to a  $5 \times 10^7 \text{ W/m}^2$  localized heat source. The minimum Nusselt number line for titanium intersects the turbulent Nusselt number correlation at a Reynolds number of about 730,000.

exist or water's viability in this case is lost.

#### 4.3.2 Free Convection Results

Since air was disqualified as a viable coolant under turbulent forced convection conditions, it follows that air is equally disqualified as the coolant under free convection conditions since these conditions have less cooling capability. Therefore, a free convection graph for air is not included. To determine what other conditions can be ruled out before graphing, the maximum Grashof numbers for each case need to be determined. Then the product of the Prandtl number and maximum Grashof number can be compared to  $10^9$  to determine if the turbulent regime needs to be considered. If the product is well below  $10^9$ , only the laminar free convection correlations need be used.

In order to calculate the maximum Grashof number, it must be broken down into its constituent parts. Namely:

$$Gr(x) = g\beta(T_s - T_\infty)x^3/\nu^2$$

where:  $g = 9.807 \text{ m/s}$  (gravitational constant) ;  $\beta$  - the volumetric expansion coefficient ( $^{\circ}\text{K}^{-1}$ ) ;  $T_s$  - temperature of the backside of the plate ( $^{\circ}\text{K}$ ) ;  $T_\infty$  - free stream temperature of the coolant ( $^{\circ}\text{K}$ ) ;  $x$  - location on the plate ( $x = 0.025 \text{ m}$  for the present work); and  $\nu$  - the kinematic viscosity ( $\text{m}^2/\text{s}$ ). The Grashof number will be at a minimum for: maximum values of  $\beta$ , minimum values of  $\nu$ , and maximum values of  $T_s - T_\infty$ .

In examining sodium first, it is found that titanium yields the largest temperature differences of  $950^{\circ}$ . The maximum  $\beta$  is approximately  $300 \times 10^{-6} (^{\circ}\text{K}^{-1})$  and the minimum  $\nu$  about  $2.36 \times 10^{-7} \text{ m}^2/\text{s}$ . These values yield an estimated maximum local Grashof number of  $7.84 \times 10^8$  and

a Prandtl-Grashof product of  $3.92 \times 10^6$ . Thus for the sodium case, only laminar correlations are used.

For the aluminum/water case ( $Pr = 1.0$ ), the local Grashof number was calculated since there was only one plate material. Thus, the value obtained would also be the maximum Grashof number. For aluminum,

$T_s - T_\infty = 600^\circ$ ;  $x = 0.025 \text{ m}$ ;  $\beta = 5.02 \times 10^{-3} (\text{K}^{-1})$  and  $\nu = 1.248 \times 10^{-7} \text{ m}^2/\text{s}$ . Therefore, maximum local Grashof number =  $2.96 \times 10^{10}$  which

also equals the Prandtl-Grashof product. Thus, both turbulent and laminar conditions must be considered.

For the titanium/water case ( $Pr = 12.0$ ),  $T_s - T_\infty = 912.5^\circ$ ;

$x = 0.025 \text{ m}$ ;  $\beta = 6.38 \times 10^{-2} (\text{K}^{-1})$ ; and  $\nu = 1.27 \times 10^{-7} \text{ m}^2/\text{s}$ . Therefore the maximum local Grashof number =  $5.53 \times 10^{11}$ . Since the Prandtl - Grashof product is obviously well over  $10^9$ , a turbulent correlation needs to be considered too. Unfortunately, only a laminar correlation was found in the literature for  $Pr > 1.0$ , so the suitability of water at  $2.152 \times 10^7 \text{ N/m}^2$  as a coolant for the titanium case had to be estimated from the aluminum/water case.

Thus with these values of Grashof number and Grashof-Prandtl products, we first decide to examine the turbulent correlation for the aluminum/water case; for if water is found to be an unsuitable coolant in the turbulent regime, it will necessarily be disqualified in the laminar regime. Therefore, in Figure 13, by noting where the maximum Grashof number is plotted on the x-axis, it is readily apparent that water is disqualified in the aluminum/water case for turbulent conditions (and thus laminar conditions). Also, for estimation purposes, the maximum Grashof for the titanium/water case is plotted on

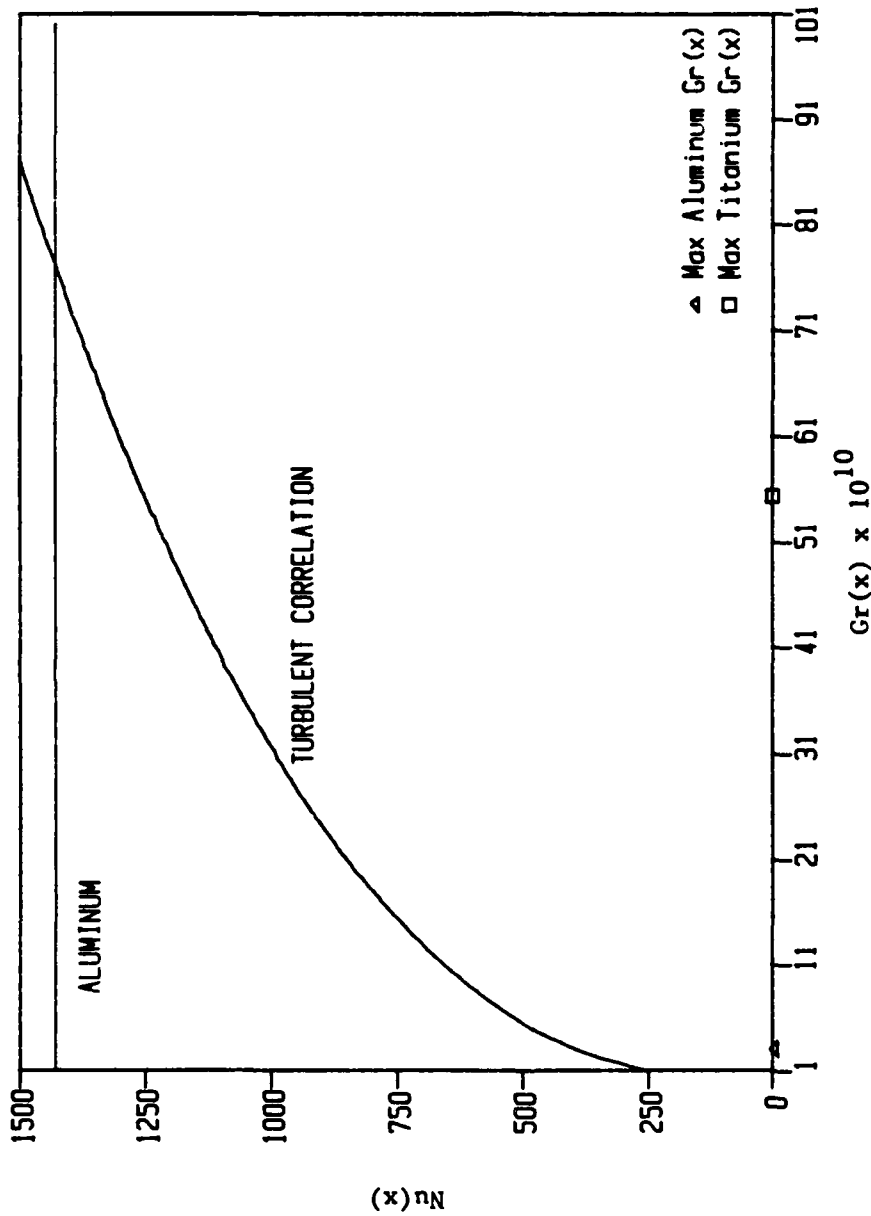


Figure 13. Nusselt number versus Grashof number for water under high pressure ( $1.235 \times 10^7 \text{ N/m}^2$ ) cooling aluminum by free convection. The minimum Nusselt number line for aluminum intersects the turbulent Nusselt number correlation line at Grashof numbers far beyond the maximum available with water even at very high pressures (as noted by the maximum Grashof number for titanium). Thus free convection cooling with water under high pressures is not feasible for this problem.

the x-axis and seen to fall well below the value needed for cooling in even the aluminum/water case. Assuming a similarity between the forced convection and free convection relative responses (which for forced convection the Reynolds numbers were within 7% of each other for the two cases), it is readily deduced that turbulent conditions will not yield the necessary cooling even for the higher Prandtl number case. For the aluminum/water case alone, an increase of Grashof number of nearly 25 times is required to qualify water as a viable coolant. It is very unlikely that the titanium/water case would be much different.

Having disqualified water under high pressure as a viable coolant, attention is turned to Figure 14 where the best chance for free convection cooling conditions lie. In order to use Figure 14 to evaluate sodium as a coolant, maximum Grashof numbers for each material have to be calculated (the estimated maximum Grashof number only defined the flow regime). Thus, for titanium:  $\beta \doteq 287.6 \times 10^{-6} (^{\circ}\text{K}^{-1})$ ;  $T_s - T_{\infty} = 950^{\circ}$ ; and  $\nu = 2.365 \times 10^{-7} \text{ m}^2/\text{s}$ . Therefore, maximum  $\text{Gr}(x) = 7.49 \times 10^8$ . For stainless steel:  $\beta \doteq 296.6 \times 10^{-6} (^{\circ}\text{K}^{-1})$ ;  $T_s - T_{\infty} = 850^{\circ}$ ;  $\nu = 2.661 \times 10^{-7} \text{ m}^2/\text{s}$ . Therefore, maximum  $\text{Gr}(x) = 5.46 \times 10^8$ . And finally for aluminum:  $\beta \doteq 270.1 \times 10^{-6} (^{\circ}\text{K}^{-1})$ ;  $T_s - T_{\infty} = 600^{\circ}$ ;  $\nu = 3.942 \times 10^{-7} \text{ m}^2/\text{s}$ . So, maximum  $\text{Gr}(x) = 1.60 \times 10^8$ . With these values calculated and plotted, Figure 14 can now be interpreted.

The conclusion readily evident from Figure 14 is that sodium is disqualified as a viable coolant for the aluminum case. The titanium case, on the other hand, makes sodium appear to be promising as a coolant. For the stainless steel case, sodium probably is not a viable coolant, since a 27.3% increase in Grashof number would be needed to prevent melting. Thus, we conclude that in the laminar free convection

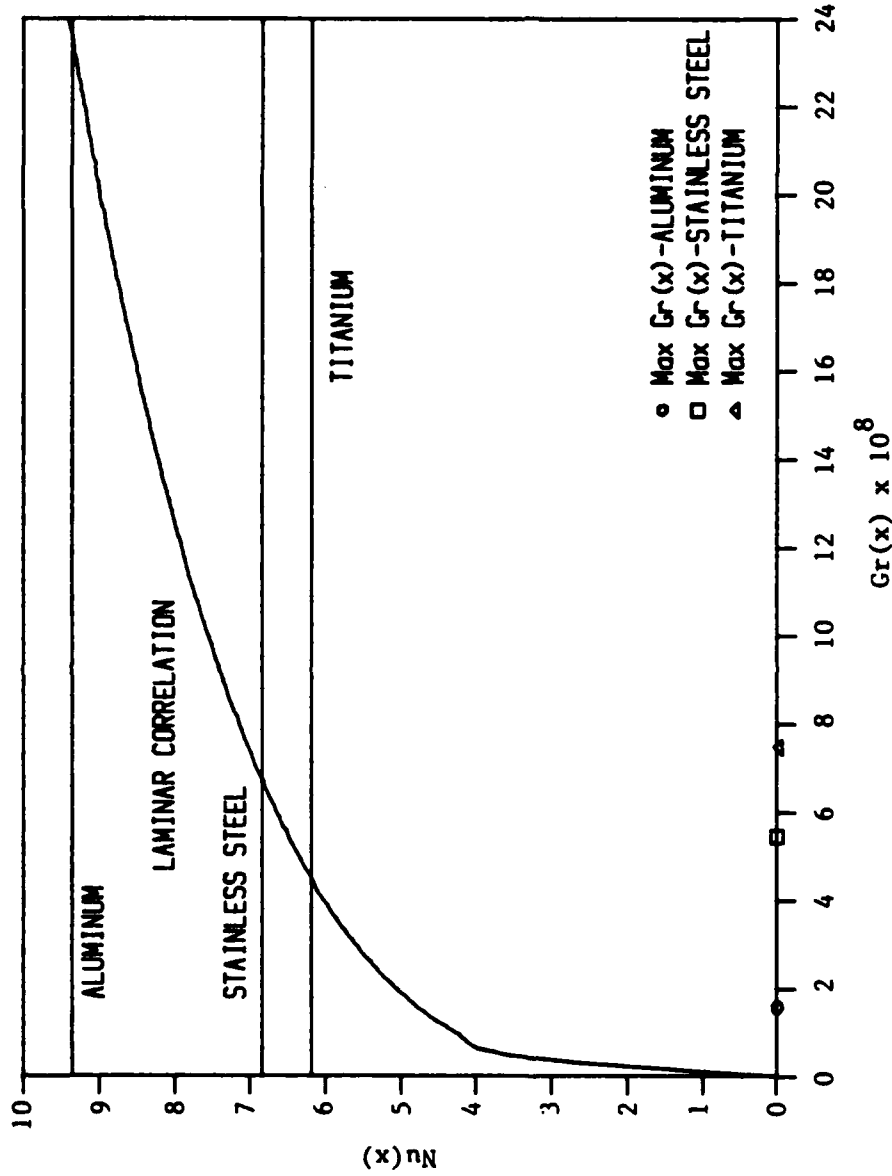


Figure 14. The combined minimum Nusselt number lines for aluminum, stainless steel, and titanium are plotted with the laminar correlation applicable to free-convection cooling with liquid sodium. Only the titanium intersection is below its corresponding maximum Grashof number. Thus, only titanium can be cooled by sodium under free convection conditions.

regime, only sodium is a viable coolant and only for a titanium plate, 0.05 m square and 0.0004 m deep, heated by a  $2 \times 10^7$  W/m<sup>2</sup> high intensity heat source localized to an  $8.125 \times 10^{-5}$  m<sup>2</sup> area in the center of the plate.

This conclusion is somewhat surprising since, judging from the typical values of heat transfer coefficient given by Incropera and DeWitt [55], a value of 14,900 W/m<sup>2</sup>·K is well into the upper ranges of typical forced convection values in liquids. However, liquid metals are definitely atypical, and the viability of sodium as a coolant for the titanium case in free convection is definitely proof of that. Any questions about the accuracy of LeFevre's correlation [62] are put to rest by Ede [64] in his comparison of LeFevre's correlation with computer solutions of the analytical problem. The final result is that the free convection cooling possibilities of the titanium/sodium combination are very good. (For a general error analysis overview, see Appendix G.)

## Chapter 5

### CONCLUSIONS AND FURTHER STUDY

#### 5.1 Conclusions

From the investigation of the basic problem of a localized high intensity heat source directed against one surface of a thin, vertical metal plate with forced or free convection cooling on the opposite surface, several conclusions can be drawn:

1. For free convection cooling, only liquid sodium is a viable coolant and only in the case of a titanium plate subjected to a  $2 \times 10^7$  W/m<sup>2</sup> heat source.
2. Sodium is a viable coolant in the turbulent forced convection regime for aluminum, titanium, and stainless steel subjected to a heat source of intensity  $2 \times 10^7$  W/m<sup>2</sup>. Velocities of no more than approximately 1 m/s are required.
3. Water under high pressure is also a viable coolant for the special cases of aluminum under an intensity of  $2 \times 10^7$  W/m<sup>2</sup> and titanium under  $5 \times 10^7$  W/m<sup>2</sup>.
4. Air is not a viable coolant for either free or forced convection regimes for any of the metals or intensities considered.
5. Heat transfer coefficient as a function of affected area has similar response curves for various intensities. In all cases, there is a rapid rise in the value of the heat transfer coefficient needed to prevent melting with initial increase in area and a just as rapid leveling off after a certain "critical" area is reached. This "critical" area occurs at smaller values of affected area for lower conductivity metals.
6. The heat transfer coefficient as a function of heat intensity produces a near-linear response in metals of high conductivity and a near exponential response for metals of low conductivity.
7. The present study appears to be unique since the literature revealed no similar studies in localized heat sources.
8. The finite element program ANSYS, by Swanson Analysis Systems, Inc., is a very accurate and versatile program that is especially suited for this study of the basic problem.

## 5.2 Further Study Recommendations

Based on the findings of the present work, recommended areas of further study are:

1. Actual experiments to test the findings of the model.
2. Investigation of the transient response to a pulsed high intensity heat source and the effect high heat transfer coefficients have on such a response.
3. Varying the location of the affected area (instead of keeping it in the center of the plate) and noting the effect on the local minimum heat transfer coefficient.
4. Investigation of the effect that a heat source with varying intensity has on the basic problem.
5. Investigation of a moving or scanning heat source.
6. Investigation of boiling as a cooling condition, and of the effect of certain surfaces to enhance boiling.
7. Examination of more materials that span a wide range of conductivities in order to establish any trends in the graph of minimum heat transfer coefficient versus conductivity.
8. Examination of the effect on minimum heat transfer coefficient when radiation is taken into account.

## APPENDIX A

## Sample Computer Program Used to Test Accuracy of ANSYS

C--The general analysis data generator is chosen.  
 /PREP7  
 /TITLE,TITANIUM SLAB--TORVIK 3RD EX.  
 C--The thermal analysis module is selected.  
 KAN,-1  
 C--The 3-D isoparametric thermal solid element (STIF 70) is chosen.  
 C This linear-approximation element has 8 nodal points with  
 C temperature being the single degree of freedom. The element is  
 C applicable to a 3-D, steady-state or transient, thermal analysis  
 C [52].  
 ET,1,70  
 C--Conductivity entered.  
 KXX,1,0.145  
 C--Density entered.  
 DENS,1,4.43  
 C--Specific heat entered.  
 C,1,0.77  
 C--Node pattern is generated  
 N,1  
 N,21,2.5  
 FILL  
 NGEN,21,21,1,21,1,,0.125  
 NGEN,5,500,1,450,1,,0.01  
 C--First element is defined.  
 E,1,2,23,22,501,502,523,522  
 C--Element sets are generated using the previously defined element(s).  
 EGEN,20,1,-1  
 EGEN,4,500,-2C  
 EGEN,20,21,-80  
 C--The absolute value of the first number after 'ITER,' is the maximum  
 C iterations for the first load step. 'TIME' = time at end of first  
 C load step. Thus, the first interval = 0.0964 - 0.0 and the intera-  
 C tion time step (ITS) = TIME/|-160|. \*  
 ITER,-160,0,160  
 TIME,0.0964  
 C--Loads are set up as step loads.  
 KBC,1  
 C--Initial temperature is defined.  
 TUNIF,300  
 C--Analysis is set up to terminate if solution does not converge.  
 CNVR,0.1,,,,1  
 C--Approximate Gaussian distribution applied to an approximate  
 circular area of 0.005m radius. The distribution is of the form:

$$F(r) = F \times \exp(-r^2/2\sigma) ; \text{ where } \sigma = 0.0025 \text{ m}$$

The values in the program were calculated by taking the radial

distance of the center of the face of each affected element and substituting that distance into the equation. The resulting values are the approximate average intensities for the affected elements. The exception is the central element which uses the peak intensity due to the nature of the Gaussian distribution.

CV,1,2,2.0E-5,1E8,,,23,22  
 CV,22,23,1.462E-5,1E8,,,44,43  
 CV,43,44,8.86E-6,1E8,,,65,64  
 CV,64,65,4.19E-6,1E8,,,86,85  
 CV,2,3,1.462E-5,1E8,,,24,23  
 CV,3,4,8.86E-6,1E8,,,25,24  
 CV,4,5,4.19E-6,1E8,,,26,25  
 CV,23,24,1.14E-5,1E8,,,45,44  
 CV,24,25,6.93E-6,1E8,,,46,45  
 CV,25,26,3.26E-6,1E8,,,47,46  
 CV,44,45,6.93E-6,1E8,,,66,65  
 CV,45,46,4.19E-6,1E8,,,67,66  
 CV,65,66,3.26E-6,1E8,,,87,86  
 C--The nodes are listed from which temperature printouts are required.  
 PRDISP,1,1,5,1  
 ,1,22,26,1  
 ,1,43,47,1  
 ,1,64,67,1  
 ,1,501,2001,500  
 C--Stress data for the last iteration is printed.  
 PRSTR,160  
 C--Stress data for the last iteration is saved for post-processing and  
 C written to File23.  
 POSTR,160  
 LWRITE  
 C--Second load step is defined. Interval = .1042-.0964  
 C ITS = 13/ (.1042-.0964)  
 ITER,13,1,1  
 TIME,0.1042  
 C--Data written to File23.  
 LWRITE  
 C--Third load step defined. Interval = .1064-.1042  
 C ITS = 1-2 / (.1064-.1042)  
 ITER,-2,1,1  
 TIME,0.1064  
 C--Data written to File23.  
 LWRITE  
 C--Fourth load step defined. Interval = .1064-.1042  
 C ITS = 1-6 / (.11 - .1064)  
 ITER,-6,1,1  
 TIME,0.11  
 C--Stress data for last iteration printed and saved  
 PRSTR,6  
 POSTR,6  
 C--Data written to File23  
 LWRITE  
 C--Complete data files written to File27.  
 AFWRIT  
 C--Exit general analysis data generator.

```
FINISH
/EXEC
C--Commence solution phase with File27 data.
/INPUT,27
FINISH
/POST26
C--Record all data for the following nodes: 1-5, 22-26, 43-47, 64-68,
C 85-89, 501, 1001, 1501, 2001.
NUMVAR,30
DISP,2,1,TEMP
DISP,3,2,TEMP
DISP,4,3,TEMP
DISP,5,4,TEMP
DISP,6,5,TEMP
DISP,7,22,TEMP
DISP,8,23,TEMP
DISP,9,24,TEMP
DISP,10,25,TEMP
DISP,11,26,TEMP
DISP,12,43,TEMP
DISP,13,44,TEMP
DISP,14,45,TEMP
DISP,15,46,TEMP
DISP,16,47,TEMP
DISP,17,64,TEMP
DISP,18,65,TEMP
DISP,19,66,TEMP
DISP,20,67,TEMP
DISP,21,68,TEMP
DISP,22,85,TEMP
DISP,23,86,TEMP
DISP,24,87,TEMP
DISP,25,88,TEMP
DISP,26,89,TEMP
DISP,27,501,TEMP
DISP,28,1001,TEMP
DISP,29,1501,TEMP
DISP,30,2001,TEMP
C--Printout the data stored over the time interval 0.06 - 0.11
C seconds in the following groupings of nodes (node numbers follow
C PRVAR).
PRTIME,0.06,0.11
PRVAR,2,3,4,5,6
PRVAR,7,8,9,10,11
PRVAR,12,13,14,15,16
PRVAR,17,18,19,20,21
PRVAR,22,23,24,25,26
PRVAR,2,27,28,29,30
FINISH
/EOF
```

\*Note: In transient thermal analysis for ANSYS, the integration time step (ITS) is related to the "conducting length" ( $\delta$ ) of an element in the region

over which the largest gradient acts (usually the length parallel to the heat flow). The larger the thermal gradient, the smaller both the ITS and  $\delta$  should be. The following guideline is given to help the user select an initial ITS for a given model:  $(ITS)_i \geq \delta^2/4\alpha$  where  $(ITS)_i$  is the initial ITS and  $\alpha$  is the material thermal diffusivity. Smaller ITS sizes (or larger elements) may cause temperature oscillations in the large temperature gradient region.

## APPENDIX B

Sample Computer Program for Determining Minimum  
Heat Transfer Coefficient

C--The general analysis data generator is chosen.  
 /PREP7  
 C--New heat transfer coefficient is selected.  
 \*SET,FILM,1.49  
 C--Title is changed to reflect new values.  
 /TITLE, TITANIUM SLAB -- FILM = 1.49  
 C--Thermal analysis module is selected.  
 KAN,-1  
 C--Choice of element type (STIF 70) is made.  
 ET,1,70  
 C--Temperature table of thermal properties is entered. Since more than  
 C 6 values a 2nd line is needed.  
 MPTEMP,1,100,200,400,600,800,1000  
 MPTEMP,7,1200,1500  
 MPDATA,KXX,1,1,0.305,0.245,0.204,0.194,0.197,0.207  
 MPDATA,KXX,1,7,0.220,0.245  
 C--Node pattern is now established.  
 N,1  
 N,21,2.5  
 FILL  
 NGEN,21,21,1,21,1,,0.125  
 NGEN,5,500,1,450,1,,,0.01  
 C--First element is defined.  
 E,1,2,23,22,501,502,523,522  
 C--More sets of elements are generated using the previous set(s) as a  
 C pattern.  
 EGEN,20,1,-1  
 EGEN,4,500,-20  
 EGEN,20,21,-80  
 C--Maximum of ten iterations is set.  
 ITER,-10,0,10  
 C--Load is defined as a step load.  
 KBC,1  
 C--Initial temperature for material properties is defined.  
 TUNIF,300  
 C--Convergence criteria of 0.1 degrees is set.  
 CNVR,0.1  
 C--Back surface of plate is assigned the heat transfer coefficient  
 C defined at the start of the program.  
 CVSF,,3,0.04,FILM,300  
 C--Front surface of plate has a  $2 \times 10^7$  W/m<sup>2</sup> intensity applied to a  
 C limited area.  
 CV,1,2,2E-5,1E8,4,1,23,22  
 CV,22,23,2E-5,1E8,25,1,44,43  
 CV,43,44,2E-5,1E8,45,1,65,64  
 CV,64,65,2E-5,1E8,65,1,86,85  
 C--Analysis is written to File27.  
 AFWRITE

```
C--General analysis data generator is exited.  
FINISH  
C--Solution phase is started with File27 data.  
/EXEC  
/INPUT,27  
FINISH  
C--The ten highest temperatures are printed out along with their  
C coordinates.  
/POST1  
SET,1  
NSORT,TEMP,,,10  
PRTEMP  
PRNODE  
FINISH  
C--ANSYS is exited.  
/EOF
```

## APPENDIX C

Minimum Heat Transfer Coefficients Necessary to Prevent Melting at Various Intensities

<u>Intensity</u> (W/m <sup>2</sup> )	<u>Aluminum</u> (W/m <sup>2</sup> ·K)	<u>Titanium</u> (W/m <sup>2</sup> ·K)	<u>SS (AISI 304)</u> (W/m <sup>2</sup> ·K)
0	0	0	0
1 × 10 <sup>7</sup>	10,500	6400	7600
2 × 10 <sup>7</sup>	28,500	14,900	17,700
3 × 10 <sup>7</sup>	47,800	25,700	30,400
4 × 10 <sup>7</sup>	68,100	40,600	48,000
5 × 10 <sup>7</sup>	89,700	67,700	81,500
6 × 10 <sup>7</sup>	112,500	130,200	165,200

## APPENDIX D

## DATA FOR FIGURES 2-4

(Note: In the listings below, the data for the lines graphed in Figures 2-4 are presented. If the data point was calculated exactly by the model, the number stands alone. Otherwise, [ ] indicates the value was extrapolated from model generated data; ( ) indicates the value was interpolated from model generated data; ( ) indicates the value was estimated from studying curve behavior. The appropriate data for each intensity is listed underneath the respective intensity across from the appropriate affected area. The left column is the area affected by the heat source in  $m^2 \times 10^{-4}$ . The values on the right underneath the intensities are heat transfer coefficients in  $W/m^2 \cdot K \times 10^4$ . Though not listed, the 0.0 heat transfer coefficient for 0.0 area is a point for each line.)

Figure 2: ALUMINUM

Area	$1 \times 10^7 W/m^2$	$2 \times 10^7 W/m^2$	$3 \times 10^7 W/m^2$
0.25 :	(0.26)	1.46	(3.30)
0.5 :	(0.72)	2.40	(4.46)
0.8125 :	1.05	2.85	4.78
1.625 :	(1.41)	3.20	(5.04)
2.4375 :	(1.53)	3.30	(5.14)
3.25 :	(1.57)	3.33	(5.18)
4.0625 :	1.59	3.34	(5.20)
	$4 \times 10^7 W/m^2$	$5 \times 10^7 W/m^2$	$6 \times 10^7 W/m^2$
	(5.20)	(7.23)	(9.34)
	(6.45)	(8.57)	[10.83]

6.81	8.97	11.25
(7.02)	(9.16)	(11.42)
(7.09)	(9.22)	(11.47)
(7.11)	(9.24)	(11.48)
(7.13)	[9.25]	11.49

Figure 3: TITANIUM

<u>Area</u>	<u><math>1 \times 10^7 \text{ W/m}^3</math></u>	<u><math>2 \times 10^7 \text{ W/m}^2</math></u>	<u><math>3 \times 10^7 \text{ W/m}^2</math></u>
0.25 :	(0.46)	1.30	(2.38)
0.375 :	-	1.41	(2.49)
0.5 :	-	1.46	(2.54)
0.8125 :	0.64	1.49	2.57
1.625 :	(0.65)	1.51	(2.58)
2.4375 :	(0.66)	1.51	(2.58)
3.25 :	(0.67)	1.51	(2.59)
	<u><math>4 \times 10^7 \text{ W/m}^2</math></u>	<u><math>5 \times 10^7 \text{ W/m}^2</math></u>	<u><math>6 \times 10^7 \text{ W/m}^2</math></u>
	(3.87)	(6.68)	12.55
	(3.98)	(6.74)	(12.67)
	(4.03)	(6.76)	(12.72)
	4.06	6.77	13.02
	(4.09)	(6.83)	(13.24)
	(4.11)	(6.89)	(13.46)
	(4.13)	[6.95]	13.68

Figure 4: STAINLESS STEEL (AISI 304)

<u>Area</u>	<u><math>1 \times 10^7 \text{ W/m}^2</math></u>	<u><math>2 \times 10^7 \text{ W/m}^2</math></u>	<u><math>3 \times 10^7 \text{ W/m}^2</math></u>
0.25 :	0.56	1.54	(2.81)
0.5 :	-	1.73	(3.00)
0.8125 :	0.76	1.77	3.04

1.625 :	(0.78)	1.79	(3.06)
2.4375 :	(0.79)	1.80	(3.07)
3.25 :	0.80	1.80	(3.08)
	<u><math>4 \times 10^7 \text{ W/m}^2</math></u>	<u><math>5 \times 10^7 \text{ W/m}^2</math></u>	<u><math>6 \times 10^7 \text{ W/m}^2</math></u>
	(4.57)	(7.46)	(14.47)
	(4.76)	(8.03)	(16.16)
	4.80	8.15	16.52
	(4.84)	(8.28)	(16.98)
	(4.89)	(8.41)	(17.44)
	(4.93)	(8.54)	[17.9]

## APPENDIX E

Minimum Heat Transfer Coefficient as a Function of Thickness  
[Results from a  $2 \times 10^7$  W/m<sup>2</sup> Local High Intensity Heat Source]

<u>Aluminum Thickness</u>	<u>Heat Transfer Coefficient</u>
(m)	(W/m <sup>2</sup> °K)
(0.0)	(31,600)*
0.0001	31,700
0.0002	30,900
0.0004	28,500
0.0008	23,100
0.0016	14,500
0.0032	6,200

\* Note: 31,600 is the theoretical heat transfer coefficient for a plate of 'zero' thickness (i.e. 100% heat conduction).  
[Included for comparison.]

## APPENDIX F

## Data for Heat Transfer Coefficients Versus Conductivity

[Values listed are for a heat source of  $2 \times 10^7 \text{ W/m}^2$ ]

<u>Conductivity</u>		<u>Heat Transfer Coefficient</u>	
(W/m °K)			(W/m <sup>2</sup> °K)
24.5*	- Titanium	-	14,900
31.7	- Stainless Steel	-	17,700
218	- Aluminum	-	28,500

\* Note: Values of conductivity are those used by the model taken from the table of values from Incropera and DeWitt [55]. In each case, the conductivity was based on the average temperature through the plate--which resulted in using the highest value in each table.

## APPENDIX G

## Error Analysis Overview

In examining the sources of error in this study, the two major sources can be identified as: the computer model itself, and the errors in the correlations used to evaluate the coolants. As noted in Table 1, the model yields an initiation of melting time only 1.45% below the exact analytical solution (computer generated). Since the model uses square elements to approximate a circular area and since the area of the model is 3.45% greater than that of the analytical solution, this lower melting time is expected. The conclusion then is that the error the model incurs when examining the metal plates heated by localized heat sources in the range of  $1 - 6 \times 10^7 \text{ W/m}^2$  appears to be approximately 1%.

One cautionary note is in order for using the model to analyze small areas at high intensities. Namely, as the affected area decreases, the number of elements available for resolving the temperature distribution decreases proportionately. Thus, if this decreased area condition is coupled with an increase in intensity, errors will be induced at the higher gradients since using too few elements to analyze a high temperature gradient situation usually yields excessively high temperatures. This is because of the linear approximations used in the finite element program. Therefore, if faced with a small area/high intensity problem, the model must have the number of elements covering the plate increased, at least in the vicinity of the area of the plate subjected to the localized heat source. For the regular version of ANSYS, this is no problem. For the educational version, with its limited memory and wave front, increasing the elements

for this problem is out of the question unless the portion of the plate being examined is decreased (i.e. invoke symmetry to reduce from 1/4 to 1/8 of the plate). This, indeed, became necessary to obtain data for intensities in the range of  $5 - 6 \times 10^7 \text{ W/m}^2$  coupled with small affected areas for the cases of titanium and stainless steel. Aluminum's high conductivity made this procedure unnecessary.

In examining the errors in the correlations used to evaluate the coolants, the literature indicates most to be under 10% (well under in many of the laminar cases). Those approaching 20% disagreement (with some of their applicable experimental data) were for air, and air was disqualified as a viable coolant under both forced and free convection conditions. Even if we remain conservative and assume a 15% error possible in the correlations, the combination of errors from the model and from the correlations still equals practically the correlation error. Thus, the coolant evaluations accomplished in this work should not be in error by much more than the uncertainty of the correlation used in each particular instance. In any case, for the correlations used in this study, no error should be greater than 15%. And, in many instances, the error will be well under 10%.

Therefore, for any user wishing to utilize this computer model to determine minimum heat transfer coefficients but supply his own correlation to evaluate cooling conditions, he can safely assume that any resultant errors equal approximately the uncertainty in the correlation.

## REFERENCES

1. Fenech, H. and Rohsenow, W.M., Thermal Conductance of Metallic Surfaces in Contact, NYP-2136, May 1959.
2. Mikic, B.B., "Thermal Contact Conductance: Theoretical Considerations", International Journal of Heat and Mass Transfer, vol. 14, pp. 205-214, 1974.
3. Ross, A.M. and Stoute, R.L., Heat Transfer Coefficient Between UO<sub>2</sub> and Zircaloy-2, CRFD-1075 : AECL-1552, 1962.
4. Rapier, A.C., Jones, T.M. and McIntosh, J.E., "The Thermal Conductance of Uranium Dioxide/Stainless Steel Interfaces", International Journal of Heat and Mass Transfer, vol. 6, pp. 397-416, 1963.
5. Cetinkale, T.N. and Fishenden, M., "Thermal Conductance of Metal Surfaces in Contact", International Heat Transfer Conference, General Discussion on Heat Transfer, Conference of the Institution of Mechanical Engineering and the American Society of Mechanical Engineers, pp. 271-275, September 1951.
6. Shlykov, Y.L., "Thermal Contact Resistance", Thermal Engineering, vol. 12, p. 102, 1966.
7. Dundurs, J. and Panek, C., "Heat Conduction Between Bodies With Wavy Surfaces", International Journal of Heat and Mass Transfer, vol. 19, pp. 731-736, 1976.
8. Suzuki, T., Hasegawa, A., Akimoto, M., Miyamoto, Y. and Katsuragi, S., The Off-Line Computation System for Supervising Performance of JOYO-JOYPAC System - Part 2, JAPFNR - 299, (Japan Atomic Energy Research Institute (Japan)), October 1976.
9. Baker, R.B., Calibration of a Fuel-to-Cladding Gap Conductance Model for Fast Reactor Fuel Pins, HEDL-TME-77-86, (Hanford Engineering Development Laboratory, Richmond, Washington (U.S.A.)), May 1978.
10. Horn, G.R. and Panisko, F.E., User's Guide For GAPCON: A Computer Program to Predict Fuel-to-Cladding Heat Transfer Coefficients in Oxide Fuel Pins, HEDL-TME-72-128, (Hanford Engineering Development Laboratory), September 1972.
11. Sudoh, T., Investigation of Typicality of Non-Nuclear Rod and Fuel-Clad Gap Effect During Reflood Phase, and Development of a FEM Thermal Transient Analysis Code HETFEM (PWR), JAERI-M-9533, (Japan Atomic Energy Research Institute, Tokai, Ibaraki), June 1981..
12. Horn, G.R. and Panisko, F.E., GAPCON: A Computer Program to Predict Fuel-to-Cladding Heat Transfer Coefficients in Oxide Fuel Pins, HEDL-TME-72-120, 1972.

13. Cook, B.A., Postirradiation Examination Data Report for Gap Conductance TEST Series, Test GC 2-3, NUREG/CR-0253, (Idaho National Engineering Laboratory, Idaho Falls (USA)), July 1978.
14. Garner, R.W., Sparks, D.T., Smith, R.H., Klink, P.H., Schwieder, D.H. and MacDonald, P.E., Gap Conductance Test Series - 2 : Test Results Report for Tests GC 2-1, GC 2-2, And GC 2-3, NUREG/CR-0300, (Idaho National Engineering Laboratory, Idaho Falls (USA)), November 1978.
15. Herziger, G., "Basic Elements of Laser Material Processing", Industrial Applications of High Power Lasers (Proceedings of SPIE - The International Society for Optical Engineering), pp. 66-74, September 1983.
16. Torvik, Peter J., A Numerical Procedure for Two Dimensional Heating and Melting Calculations. With Application to Laser Effects, AFIT-TR 72-2, (Air Force Institute of Technology, Wright-Patterson AFB, OH), March 1972.
17. Garnier, J.E. and Begej, S., Ex-Reactor Determination of Thermal Gap and Contact Conductance Between Uranium Dioxide: Zircaloy-4 Interfaces, Stage I : Low Gas Pressure. NUREG/CR-0330, PNL-2696; (Pacific Northwest Laboratory), April 1979.
18. Garnier, J.E. and Beg-j, S., Ex-Reactor Determination of Thermal Gap Conductance Between Uranium Dioxide and Zircaloy-4, Stage II: High Gas Pressure, NUREG/CR-0330, PNL-3232 (Vol. 2), (Pacific Northwest Laboratory), June 1980.
19. Parker, W.J., Jenkins, R.J., Butler, C.P. and Abbott, G.L., "Flash Method of Determining Thermal Diffusivity, Heat Capacity, and Thermal Conductivity", Journal of Applied Physics, vol. 32, no. 9, pp. 1679-1684, September 1961.
20. Peckham, G., "A New Method for Minimising a Sum of Squares without Calculating Gradients", The Computer Journal, vol. 13, no. 4, pp. 418-420, November 1970.
21. Suzuki, T., Hasegawa, A., Akimoto, M., Miyamoto, Y. and Katsuragi, S., The Off-Line Computation System for Supervisory Performance of JOYO : JOYPAC System 2, JAERI-1247, (Japan Atomic Energy Research Institute, Tokai, Ibaraki), October 1976.
22. Baker, R.B., Calibration of a Fuel-to-Cladding Gap Conductance Model for Fast Reactor Fuel Pins, HEDL-TME-77-86, (Hanford Engineering Development Laboratory, Richland, Washington), May 1978.
23. Ross, A.M. and Stoute, R.D., Heat Transfer Coefficient Between UO<sub>2</sub> and Zircaloy-2, AECL-1552, June 1962.
24. Dutt, D.S. and Baker, R.B., A Correlated Code for the Prediction of

Liquid Metal Fast Breeder Reactor (LMFBR) Fuel Thermal Performance,  
HEDL-TME-74-55, June 1975.

25. Meek, C.C., Adams, W.J. and Doerner, R.C., "Determination of Fuel-Clad Thermal Gap Conductance by Use of Kalman Filter Methods", Nuclear Science and Engineering, vol. 81, pp. 560-562, August 1982.
26. Badger, W.L. and McCabe, W.L., Elements of Chemical Engineering, McGraw-Hill Book Co., New York, NY, 1936.
27. Roberts, E., Balfour, M.G., Hopkins, G.W., Smalley, W.R. "Fuel Modeling and Performance of High Burnup Fuel Rods", Water Reactor Fuel Performance (AHS Topical Meeting), pp. 133-143, May 9-11, 1977.
28. Todreas, N. and Jacobs, G., "Thermal Contact Conductance in Reactor Fuel Elements", Nuclear Science and Engineering, vol. 50, pp. 283-290, 1973.
29. Marr, William W., "COBRA-3M : A Modified Version of COBRA for Analyzing Thermal-Hydraulics in Small Pin Bundles", Nuclear Engineering and Design, vol. 53, pp. 223-235, 1979.
30. Nguyen-Minh, Than and Neuer, Gunther, "Measurement of Thermal Gap Resistance and Contact Resistance by the Modulated Heating Method," High Temperatures - High Pressures, vol. 13, pp. 113-118, 1981.
31. Golodenko, N.N. and Kuz'michev, V.M., "Thermal Processes in Metals Irradiated by Powerful Laser Pulses", High Temperature, vol. 10, no. 5, pp. 1013-1015, September-October 1972.
32. Locke, Edward V., Hoag, Ethan D. and Hella, Richard A., "Deep Penetration Welding with High-Power CO<sub>2</sub> Lasers", IEEE Journal of Quantum Electronics, vol. QE-8, no. 2, pp. 132-135, February 1972.
33. Hablanian, M.H., "A Correlation of Welding Variables", Proceedings of the 4th Symposium of Electron Beam Technology, 1962.
34. Torvik, Peter J., Some Further Numerical Studies of Laser Induced Melting and Vaporization, AFIT TR 73-1, (Air Force Institute of Technology, Wright-Patterson A.F.B., OH), January 1973.
35. Paek, Un-Chul and Gagliano, Francis P., "Thermal Analysis of Laser Drilling Processes", IEEE Thermal of Quantum Electronics, vol. QE-8, no. 2, pp. 112-119, February 1972.
36. Prokhorov, A.M., Batanov, V.A., Bunkin, F.V. and Fedorov, V.B., "Metal Evaporation Under Powerful Optical Radiation", IEEE Journal of Quantum Electronics, vol. QE-9, no. 5, pp. 503-510, May 1973.
37. Anisimov, S.I., Imas, Y.A., Romanov, G.S. and Hodiko, Y.V., "Interaction Between High Power Radiation and Metal", Moscow: Nauka, 1970.

38. Jones, Marshall G. and Wang, Hsin-Pang, "Experimental Evaluation and Finite Element Analysis of Laser Welded Copper - Copper and Copper - Aluminum Joints", *Advances in Laser Engineering and Applications (SPIE Proceedings)*, vol. 247, pp. 45-54, July 31 - August 1, 1980.
39. Blottner, F.G., Thermal Modeling of Laser Welding with a Quasi-One-Dimensional Approach, SAND-83-1120C (DE 84 001292), (Sandia National Laboratory, Albuquerque, NM), 1983.
40. Decker, I., Ruge, J. and Atzert, U., "Physical Models and Technological Aspects of Laser Gas Cutting", *Industrial Applications of High Power Lasers (SPIE Proceedings)*, vol. 455, pp. 81-87, September 26-27, 1983.
41. Masters, J.I., "Problems of Intense Surface Heating of a Slab Accompanied by a Change of Phase", *Journal of Applied Physics*, vol. 27, pp. 477-484, 1956.
42. Dewey, C.F., Schiesinger, S.J. and Sashkin, L., "Temperature Profiles in a Finite Solid with Moving Boundary," *Journal of the Aero-Space Sciences*, vol. 27, pp. 59-64, 1960.
43. Hanley, Stephen T., A General Solution to the One and Two Dimensioned Melting Using a Finite Difference Approach, NRL Report 7200, Naval Research Labs, 1970.
44. DeWitt, Robert N., Radial Heat Conduction in Laser Heating of Material Slabs, NRL Report 7314, (Naval Research Labs), 1971.
45. Mazumder, J. and Steen, W.M., "Heat Transfer Model for CW Laser Material Processing", *Journal of Applied Physics*, vol. 51, no. 2, pp. 941-947, February 1980.
46. Wilson, Edward L. and Nickell, Robert E., "Application of the Finite Element Method to Heat Conduction Analysis", *Nuclear Engineering and Design*, vol. 4, pp. 276-286, 1966.
47. Friedman, E., Finite Element Analysis of Arc Welding, WAPD-TM-1430, (Bettis Atomic Power Laboratory, West Mifflin, PA), January 1980.
48. Upson, C.D., Gresho, P.M., Sani, R.L., Chan, S.T. and Lee, R.L., A Thermal Convection Simulation in Three Dimensions by a Modified Finite Element Method, UCRL-85555, (Lawrence Livermore National Laboratory, CA), 21 July, 1981.
49. Glickstein, S.S. and Friedman, E., "Weld Modeling Applications", *Welding Journal*, vol. 63, pp. 38-42, September 1984.
50. Irons, B.M., "A Frontal Solution Program for Finite Element Analysis", *International Journal for Numerical Methods in Engineering*, vol. 2, no. 1, January 1970, pp. 5-23 (Discussion, May 1970, p. 149).

AD-A170 856

MODEL SIMULATION OF A LOCALIZED HIGH INTENSITY HEAT  
SOURCE INTERACTING W/ (U) AIR FORCE INST OF TECH  
WRIGHT-PATTERSON AFB OH F H CRANFILL 1986

2/2

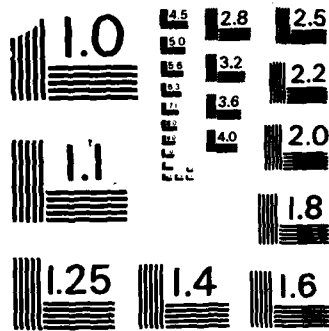
UNCLASSIFIED

AFIT/CI/NR-86-87T

F/G 18/9

NL





MICROCOPY RESOLUTION TEST CHART  
NATIONAL BUREAU OF STANDARDS-1963-A

51. Melosh, R.J. and Bamford, R.M., "Efficient Solution of Load-Deflection Equations", Journal of the Structural Division, ASCE, vol. 95, no. ST4, Proceedings Paper 6510, April 1969, pp. 661-676 (Discussions, December 1969; January, February, May, 1970; Closure, February, 1971).
52. DeSalvo, G.J. and Swanson, J.A., ANSYS Engineering Analysis System User's Manual, Swanson Analysis Systems, Inc., Houston, PA, March 1, 1983.
53. Kohnke, P.C., ANSYS Theoretical Manual, Swanson Analysis Systems, Inc., Houston, PA, February 1, 1983.
54. Olcer, N.Y., "General Solutions to a Class of Heat Flow Problems in a Finite Circular Cylinder", British Journal of Applied Physics, vol. 18, pp. 89-105, 1967.
55. Incropera, F.P. and DeWitt, D.P., Fundamentals of Heat Transfer, John Wiley and Sons, Inc., New York, 1981.
56. Touloukian, Y.S. and Ho, C.Y., Eds., Thermo-physical Properties of Matter. The TPRC Data Series, Plenum Publishing Corporation, New York; vol. 1, Thermal Conductivity of Metallic Elements and Alloys; vol. 3, Thermal Conductivity of Nonmetallic Liquids and Alloys; vol. 6, Specific Heat of Nonmetallic Liquids and Gases; vol. 11, Viscosity; 1975.
57. Kays, W.M. and Crawford, M.E., Convective Heat and Mass Transfer (2nd Ed.), McGraw-Hill Book Co., New York, 1980.
58. Fujii, T. and Fujii, M., "The Dependence of Local Nusselt Number on Prandtl Number in the Case of Free Convection Along A Vertical Surface with Uniform Heat Flux", International Journal of Heat Mass Transfer, vol. 19, pp. 121-122, 1976.
59. Churchill, S.W. and Ozoe, H., "A Correlation for Laminar Free Convection from a Vertical Plate", Journal of Heat Transfer, Series C, vol. 95, pp. 540-541, November 1973.
60. Vliet, G.C. and Ross, D.C., "Turbulent Natural Convection on Upward and Downward Facing Inclined Constant Heat Flux Surfaces", Journal of Heat Transfer, Series C, vol. 97, pp. 549-554, November 1975.
61. Vliet, G.C. and Liu, C.K., "An Experimental Study of Turbulent Natural Convection Boundary Layers", Journal of Heat Transfer, Series C, vol. 91, pp. 517-531, November 1969.
62. LeFevre, E.J., "Laminar Free Convection from a Vertical Plane Surface", Proceedings of the 9th International Congress on Applied Mechanics, Brussels, vol. 4, p. 168, 1956.
63. Churchill, S.W. and Usagi, R., "A General Expression for the Correlation of Rates of Transfer and Other Phenomena", AIChE Journal, vol. 18, no. 6, pp. 1121-1128, November 1972.

64. Ede, A.J., "Advances in Free Convection", Advances in Heat Transfer, vol. 4, Academic Press, New York, pp. 1-64, 1967.
65. Bayley, F.J., "An Analysis of Turbulent Free-Convection Heat-Transfer", Institution of Mechanical Engineers' Proceedings, vol. 169, pp. 361-368, 1955.
66. Eckert, E. and Jackson, T.W., Analysis of Turbulent Free Convection Boundary Layer on Flat Plate, N.A.C.A. Report 1015, 1950.
67. Pitts, D.R. and Sissom, L.E., Theory and Problems of Heat Transfer, Schaum's Outline Series, McGraw-Hill Book Company, New York, 1977.
68. Warner, C.Y. and Arpaci, V.S., "An Experimental Investigation of Turbulent Natural Convection in Air at Low Pressure along a Vertical Heated Flat Plate", International Journal of Heat & Mass Transfer, vol. 11, pp. 397-406, 1968.
69. Fujii, T., Takeuchi, M., Fujii, M., Suzaki, K. and Uehara, H., "Experiments on Natural-Convection Heat Transfer from the Outer Surface of a Vertical Cylinder to Liquids", International Journal of Heat & Mass Transfer, vol. 13, pp. 753-787, 1970.
70. Churchill, S.W. and Chu, H.H.S., "Correlating Equations for Laminar and Turbulent Free Convection From a Vertical Plate", International Journal of Heat and Mass Transfer, vol. 18, pp. 1323-1329, 1975.
71. Jaluria, Yogesh, "Natural Convection-Heat & Mass Transfer", HMT - The Science & Applications of Heat & Mass Transfer, vol. 5, Pergamon Press, New York, 1980.
72. Eckert, E.R.G. and Drake, R.M., Jr., Analysis of Heat and Mass Transfer, McGraw-Hill Book Co., Inc., New York, 1972.
73. Eckert, E.R.G. and Drake, R.M., Jr., Heat and Mass Transfer, 2nd Ed., McGraw-Hill Book Co., Inc., New York, 1959.

## VITA

The author was born June 2, 1955 in Lexington, Kentucky. He was awarded a four-year scholarship by the United States Air Force in 1973 to attend the University of Kentucky in Lexington, Kentucky. In May of 1977, the author received a Bachelor of Science degree in Mechanical Engineering from the University of Kentucky and a commission from the United States Air Force. He trained as a navigator in the B-52G bomber and later upgraded to a radar navigator/bombardier. During his 5 1/2 years in an operational squadron, he obtained an instructor rating in both radar navigator and navigator positions. In October of 1983, he was selected by the Commander in Chief of the Strategic Air Command to return to a civilian university to pursue a Master of Science degree in Nuclear Engineering. Thus, in August of 1984, he returned to the University of Kentucky to pursue the Master of Science degree.

*Frank Mark Cuniff*

*30 May 1986*

END

DTIC

9-86